

**Best  
Available  
Copy**

AD-785 234

ARPA-NRL LASER PROGRAM

J. R. Airey, et al

Naval Research Laboratory  
Washington, D. C.

July 1974

DISTRIBUTED BY:

**NTIS**

**National Technical Information Service  
U. S. DEPARTMENT OF COMMERCE  
5285 Port Royal Road, Springfield Va. 22151**

UNCLASSIFIED

SECURITY CLASSIFICATION OF THIS PAGE (When Data Entered)

AD-785234

REPORT DOCUMENTATION PAGE		READ INSTRUCTIONS BEFORE COMPLETING FORM
1. REPORT NUMBER NRL Memorandum Report 2846	2. GOVT ACCESSION NO.	3. RECIPIENT'S CATALOG NUMBER
4. TITLE (and Subtitle) ARPA-NRL Laser Program - Semiannual Technical Report to Defense Advanced Research Projects Agency 1 July 1973 - 31 December 1973		5. TYPE OF REPORT & PERIOD COVERED A semi-annual technical report; work continuing
7. AUTHOR(s) Laser Physics Branch		6. PERFORMING ORG. REPORT NUMBER
9. PERFORMING ORGANIZATION NAME AND ADDRESS Naval Research Laboratory Washington, D.C. 20375		8. CONTRACT OR GRANT NUMBER(s)
11. CONTROLLING OFFICE NAME AND ADDRESS Defense Advanced Research Projects Agency Washington, D.C. 20375		10. PROGRAM ELEMENT, PROJECT, TASK AREA & WORK UNIT NUMBERS NRL Prob. 55N01-21, R08-45, K03-53 Project No. 2E20
14. MONITORING AGENCY NAME & ADDRESS (if different from Controlling Office)		12. REPORT DATE July 1974
		13. NUMBER OF PAGES 64
		15. SECURITY CLASS. (of this report) UNCLASSIFIED
		15a. DECLASSIFICATION/DOWNGRADING SCHEDULE
16. DISTRIBUTION STATEMENT (of this Report)  Approved for public release; distribution unlimited.		
17. DISTRIBUTION STATEMENT (of the abstract entered in Block 20, if different from Report)		
18. SUPPLEMENTARY NOTES		
19. KEY WORDS (Continue on reverse side if necessary and identify by block number)  Lasers Electrical Lasers Chemical Lasers  Reproduced by NATIONAL TECHNICAL INFORMATION SERVICE U.S. Department of Commerce Springfield, VA 22151		
20. ABSTRACT (Continue on reverse side if necessary and identify by block number) The ARPA-NRL High Energy Laser Program is concerned with the development of laser technology in three project areas: Chemical Infrared Lasers, Electrical Infrared Lasers and Electronic State Lasers. The Chemical Infrared Laser Program is concerned with the development of the DF-CO <sub>2</sub> supersonic transfer chemical laser, the study of the CO vibrational distribution from exothermic reactions which produce CO and the measurement of energy transfer rates of CO. The objective of the DF-CO <sub>2</sub> program is the chemical augmentation of gasdynamic CO <sub>2</sub> lasers. Detailed measurements of the initial vibrational distribution from		

DD FORM 1 JAN 73 1473

EDITION OF 1 NOV 65 IS OBSOLETE  
S/N 0102-014-6601

(Abstract continues)

i

UNCLASSIFIED  
SECURITY CLASSIFICATION OF THIS PAGE (When Data Entered)

UNCLASSIFIED

SECURITY CLASSIFICATION OF THIS PAGE(When Data Entered)

20. (Continued Abstract)

the  $O + CS$  reaction indicate that this process is unlikely to produce efficient CO laser action at wavelengths  $< 5 \mu$ . V-V and V-R,T energy transfer rates have been measured for CO-additive mixtures and the temperature dependence of some of these rates has been investigated.

The Electrical Infrared Laser Program consists of two primary projects, short-pulse  $CO_2$  laser technology and electric-discharge gasdynamic lasers (EDGDL). The short pulse  $CO_2$  laser has achieved 70 J in a single 1 nsec pulse. Advances in pulse switch out technology and measurements of gain profiles and spectral content are reported. Components for an EDGDL apparatus for the investigation of the  $D_2^* - HCl$  transfer laser have been fabricated and are being assembled.

UNCLASSIFIED

SECURITY CLASSIFICATION OF THIS PAGE(When Data Entered)

## TABLE OF CONTENTS

FOREWORD.....	
CHEMICAL INFRARED LASER PROGRAM.....	1
DF-CO <sub>2</sub> SUPERSONIC TRANSFER CHEMICAL LASER (TCL).....	1
CO VIBRATIONAL DISTRIBUTION STUDIES.....	4
CARBON MONOXIDE ENERGY TRANSFER STUDIES.....	4
ELECTRICAL INFRARED LASERS.....	12
SHORT PULSE CO <sub>2</sub> MOLECULAR LASER.....	12
Short Pulse Oscillator.....	12
Small Signal Amplifiers (Pre-Amps).....	14
Large Aperture Amplifiers.....	15
Excessive Jitter of Gain Pulse.....	15
Unreliable Triggering of Main Marx.....	16
Cathode Support Structure Failure.....	16
Capacitor Failure.....	16
Pulse Amplification Experiments.....	17
Conclusions.....	18
ELECTRIC DISCHARGE GASDYNAMIC LASER, EDGDL.....	19
ELECTRONIC STATE LASERS.....	33
ELECTRON BEAM INITIATED VISIBLE TRANSITION LASERS.....	33
DOUBLE-PULSE EXCITATION TECHNIQUES.....	35
VISIBLE CHEMICAL LASER EXPERIMENTS.....	36

TABLE OF CONTENTS

APPENDIX A - QUANTITATIVE LASER MEASUREMENT OF VERY SMALL ABSORPTIONS:

STUDIES OF THE  $C + CS \rightarrow CO(V) + S$  REACTION..... A-1



## FOREWORD

The Laser Physics Branch of the Optical Sciences Division, Naval Research Laboratory, Washington, D. C., prepared this semiannual report on work sponsored by the Advanced Research Projects Agency, ARPA Order 2062. Co-authors of the report were J.R. Airey, L. Champagne, N. Djeu, W.H. Green, J.K. Hancock, M.C. Lin, F. O'Neill, S.K. Searles, J.A. Stregack, W.S. Watt, B. Wexler, W. Whitney.

SEMIANNUAL TECHNICAL REPORT

REPORTING PERIOD

1 July 1973 - 31 December 1973

1. DARPA Order	2062
2. Program Code Number	2E20
3. Name of Contractor	Naval Research Laboratory
4. Effective Date of Contract	1 July 1972
5. Contract Expiration Date	30 June 1974
6. Amount of Contract	\$590,000
7. Contract Number	63201D
8. Principal Investigator	J.R. Airey
9. Telephone Number	(202) 767-3217
10. Project Scientist	W.S. Watt
11. Telephone Number	(202) 767-2028
12. Title of Work	High Power Lasers

SPONSORED BY

DEFENSE ADVANCED RESEARCH PROJECTS AGENCY

DARPA Order No. 2062



## CHEMICAL INFRARED LASER PROGRAM

### 1. DF-CO<sub>2</sub> SUPERSONIC TRANSFER CHEMICAL LASER (TCL)

The DF-CO<sub>2</sub> laser operates in the 10  $\mu$  CO<sub>2</sub> band as a result of the highly efficient transfer of energy from vibrationally excited DF to the asymmetric stretching mode of CO<sub>2</sub>. The vibrational states of DF are preferentially excited during its chemical formation. Although hydrogen halide chemical lasers typically operate at 10 torr pressure, the introduction of the vibrational energy transfer process to CO<sub>2</sub> allows operation at much higher pressure. This feature coupled with a supersonic flow offers the possibility of atmospheric pressure recovery. Thus the DF-CO<sub>2</sub> TCL is of interest both as a chemical laser operating without pumps and as a means of upgrading gasdynamic CO<sub>2</sub> lasers by the addition of chemical energy to the flow.

The principle of the NRL DF-CO<sub>2</sub> supersonic TCL, the apparatus acquisition and modification, and the mode of operation both as a chemical laser and gasdynamic laser have been described in previous reports. (1-4) At the end of the last reporting period, changes to the optical cavity were discussed. The purpose of these cavity changes is as follows. If the D<sub>2</sub>-F<sub>2</sub> reaction takes place only near the nozzles then a high gain region will result in that location with low gain or loss regions further downstream in the cavity. The result of the chemistry would then only have a small effect on the output of the 8" long cavity. The use of smaller optics nearer the nozzle array would clearly take more advantage of high-gain regions produced by the chemical reactions.

With this new optical cavity arrangement, power output data have been obtained at locations 2 cm and 10 cm downstream of the nozzle exit. These data illustrate two important findings. First, the small amount of HF produced by F atoms reacting with the pilot-produced water vapor, has a large deactivating effect. More importantly however, DF produced by reaction of F atoms with D<sub>2</sub> has been demonstrated to pump the CO<sub>2</sub> and to increase the lasing output.

The effect of HF deactivation is clearly seen in Figure 1. In this case the device operates as a gasdynamic laser with a period during which fluorine is injected into the combustor. The output during

---

(1-4) ARPA-NRL Laser Program Semiannual Technical Reports, 1 July 1971 - 30 June 1973, NRL Memorandum Reports Nos. 2483, 2529, 2654, 2767.

fluorine addition, region 2, is seen to be about 60% of that for the gasdynamic laser, region 1. The power reduction was found to be proportional to the amount of fluorine added and its dependence on temperature was in the same direction as the deactivation of  $\text{CO}_2$  by HF. Thus these observations lead to the conclusion that the combustor produced HF is a serious problem.

As a result of these findings, a considerable amount of research was undertaken to reduce this effect. To be brief, it was found that the gasdynamic laser operates best with near the minimum amount of hydrogen bearing species to catalyse the CO oxidation. The use of deuterium as  $\text{D}_2/\text{O}_2$  rather than  $\text{CH}_4/\text{O}_2$  as the pilot gas did not materially reduce the deactivation and was not as effective as a pilot fuel.  $\text{CD}_4$ , which would be the best pilot fuel for the current combustor was not evaluated due to the expense of procuring it.

While other species, such as NO and  $\text{NO}_2$ , which do not contain hydrogen have been proposed as catalysts for the oxidation of CO to  $\text{CO}_2$  there is little information available. Rather than going into an extensive program of combustor optimization it was decided to continue with experiments to investigate whether chemical pumping as a result of DF formation was occurring.

The output from a gasdynamic laser to which fluorine was added to the combustion region and deuterium was added at the nozzle throat is shown in Figure 2. Again, as in Figure 1, region 1 denotes the period of gasdynamic laser performance and region 2 denotes the time when fluorine is added to the flow. Region 3 corresponds to the time during which both fluorine and deuterium was flowing. It is clear that the result of adding deuterium is to raise the output power back to its level during purely gasdynamic laser operation.

The only plausible explanation for the improved performance with deuterium addition, is that vibrationally excited DF is formed and transfers its energy to the  $\text{CO}_2$ . Thus these results offer a definitive proof of the chemical augmentation of a gasdynamic laser. In fact, if one considers the augmentation to be from the level during region 2, increases in the laser output by a factor of 3-4 have been observed as a result of chemical pumping.

The amount of pumping during the deuterium-on cycle is greater for larger mass flow rates of fluorine and can be optimized by varying the deuterium delivery pressure. No temperature dependence of the effect was observed.

The effect of HF deactivation and DF pumping have been investigated for a variety of experimental conditions and gas flow-rates at two positions in the optical cavity region. These locations are 2.5 cm and 10 cm

downstream of the nozzle-exit plane. For a given set of gas flow conditions, the deactivation by HF was greater at 10 cm downstream. This indicates deactivation in the cavity as well as in the nozzle region.

The effect of DF pumping was almost independent of the location. This latter result, on its own, could have been interpreted as simply due to inefficient mixing of the  $D_2$  stream into the main flow. However, it has also been observed that the temperature in the combustor rises when large amounts of  $D_2$  are injected into the flow. This suggests that a substantial fraction of the  $F/D_2$  chemistry is occurring in the subsonic region and will continue during the nozzle expansion. The early chemistry has several effects. Apart from heating the gas flow, it reduces the available chemical pumping and increases the ground state DF which serves as additional deactivating species.

These results appear to indicate that the present nozzle design is unlikely to lead to significant chemical pumping of a  $CO_2$  GDL. Accordingly, in collaboration with Bell Aerospace Company, a nozzle is being built that allows  $D_2$  injection at the tips of the nozzle blades. This nozzle will be delivered about 1 March and tested during the remainder of FY-74. In addition, a scanning-gain apparatus is being assembled. This will be used to measure the gain at  $10.6 \mu$  as a function of distance in the flow direction during a single experiment. Check-out of this apparatus and preliminary experiments with the existing nozzle will be completed before the Bell nozzle is delivered.

In parallel with the experimental program, a number of computer modeling calculations of the chemically augmented gasdynamic  $CO_2$  laser have been carried out. These have been done in conjunction with Bell Aerospace Company using their computer program. This computer code has successfully modeled the previous subsonic DF- $CO_2$  work of Cool and of Falk.

The calculations indicate the potential of chemical augmentation but reveal a strong dependence on where the mixing of the reactants occurs. The predicted gain profiles for a variety of combustor operating conditions have been used to guide the experimental program. These conditions closely match those where the largest chemical pumping occurs but the observed pumping is much less than the calculations predict. However if pre-reaction in the combustor is included in the calculations, the predicted chemical augmentation is reduced accordingly.

With the Bell nozzle, pre-reaction is avoided and the measured and predicted gain profiles can be compared directly.

## 2. CO VIBRATIONAL DISTRIBUTION STUDIES

The intracavity laser probing technique has been further improved and shown to have a detectivity of 0.01% gain-loss with the present CO laser. Using this technique the vibrational distribution of CO produced from O and CS in a fast-flow intracavity reactor has been measured. As a result of the improved sensitivity an essentially unrelaxed CO vibrational distribution was obtained with a total CO concentration of  $\sim 2 \times 10^{13} \text{cm}^{-3}$ . The distribution is peaked at  $V=12$  and drops to  $\sim 10\%$  at  $V=5$  and  $V=16$ . The populations for  $V < 5$  and  $V > 16$  are negligible.

The details of the probing technique and the measurements of the  $\text{CO} + \text{S}$  reaction are described in Appendix A which has been accepted for publication in the Journal of Chemical Physics.

The system is being modified to probe the  $\text{CH} + \text{O}_2 \rightarrow \text{CO}(V) + \text{OH}$  reaction.

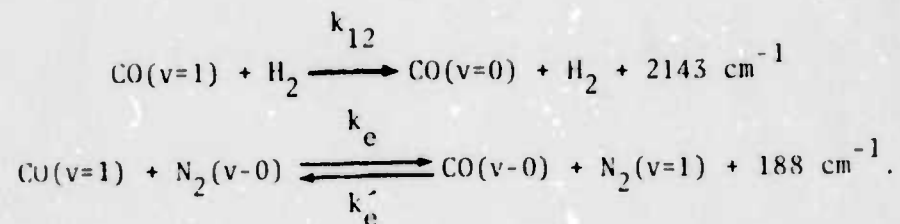
## 3. CARBON MONOXIDE ENERGY TRANSFER STUDIES

The use of a frequency doubled  $\text{CO}_2$  laser to vibrationally excite CO molecules has led to the measurement of  $\text{CO}(v=1)$  additive quenching rates at room temperature.<sup>(1)</sup> Because of the speed and selectivity of near resonant  $V \rightarrow V$  energy transfer in CO mixtures vibrational quenching information from certain additive molecules have been obtained. Deactivation rates have been measured for  $\text{D}_2(v=1)$ ,  $\text{CO}_2(001)$ ,  $\text{N}_2\text{O}(001)$ ,  $\text{OCS}(001)$ ,  $\text{CS}_2(001)$ , and  $\text{C}_2\text{N}_2(00100)$  using this technique.<sup>(1,2)</sup>

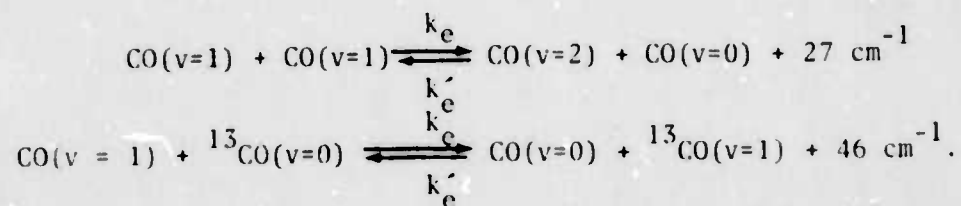
A summary of recently measured  $V \rightarrow V$ ,  $V \rightarrow R,T$  energy transfer rates in CO-additive mixtures is given in Table 1. The reported rates for  $V \rightarrow V$  transfer and subsequent  $V \rightarrow R,T$  deactivation in  $\text{CO}^+ - \text{CS}_2$  and  $\text{CO}^+ - \text{OCS}$  suggest that lasing in  $\text{CS}_2$  at  $11.5 \mu\text{m}$  and  $\text{OCS}$  at  $8.30 \mu\text{m}$  is possible using the transfer of vibrational energy from excited CO molecules. Lasing in  $\text{CS}_2$  has recently been demonstrated at Mathematical Sciences Northwest using e-beam excitation of CO.

In addition to the room temperature results,  $\text{CO-H}_2$  and  $\text{CO-N}_2$  rate measurements have been completed over the temperature range  $100\text{-}600^\circ\text{K}$  (see Figures 3 and 4). The processes studied were:

1. W.H. Green and J.K. Hancock, J. Chem. Phys. 59, 4326 (1973).
2. J.K. Hancock, D.F. Starr and W.H. Green, manuscript in preparation.



Preliminary data have also been obtained over the 200-500°K range for the following (see Figure 5).



These and future temperature studies are intended to provide rate data of import to electrical and chemical CO lasers, and to test the validity of high temperature V → V data tediously extracted from shock tube measurements.



COLLISION PROCESS	ENERGY DEFECT $\Delta E(\text{cm}^{-1})$	RATE CONSTANT ( $\text{sec}^{-1} \text{ torr}^{-1}$ )	COLLISION PER Deactivation	CROSS SECTION ( $\text{\AA}^2$ )
CO(2) + CO(0)	-27 $\text{cm}^{-1}$	(1.08 $\pm$ 0.03) $\times 10^5$	84.7	0.506
CO(1) + SO <sub>2</sub>	781	11.6 $\pm$ 0.2	7.41 $\times 10^5$	6.44 $\times 10^{-5}$
CO(1) + CS <sub>2</sub>	510	(1.49 $\pm$ 0.17) $\times 10^4$	6.23 $\times 10^2$	0.0846
CO(1) + N <sub>2</sub> O	-81	(1.51 $\pm$ 0.13) $\times 10^5$	56.2	0.783
CO(1) + OCS	81	(2.57 $\pm$ 0.48) $\times 10^5$	33.9	1.40
CO(1) + C <sub>2</sub> N <sub>2</sub>	-15	> 2 $\times 10^6$	< 5	> 11
N <sub>2</sub> O(001) + CO	2224 $\text{cm}^{-1}$	(4.85 $\pm$ .07) $\times 10^2$	1.75 $\times 10^4$	2.52 $\times 10^{-3}$
+ N <sub>2</sub> O		(7.55 $\pm$ .13) $\times 10^2$	1.02 $\times 10^4$	4.44 $\times 10^{-3}$
+ Ar		(1.22 $\pm$ .26) $\times 10^2$	5.8 $\times 10^4$	7.0 $\times 10^{-4}$
OCS(001) + CO	2062	(1.05 $\pm$ .28) $\times 10^4$	8.29 $\times 10^2$	0.0575
OCS		(4.66 $\pm$ .64) $\times 10^4$	1.65 $\times 10^2$	0.320
Ar		(1.43 $\pm$ .06) $\times 10^3$	5.01 $\times 10^3$	8.78 $\times 10^{-3}$
CS <sub>2</sub> (001) + CO	1533	(7.40 $\pm$ 1.5) $\times 10^2$	1.25 $\times 10^4$	4.20 $\times 10^{-3}$
+ CS <sub>2</sub>		(2.15 $\pm$ .35) $\times 10^3$	3.82 $\times 10^3$	0.0166
C <sub>2</sub> N <sub>2</sub> (00100) + CO	2158	(3.23 $\pm$ 0.08) $\times 10^3$	2.97 $\times 10^3$	0.0173
+ C <sub>2</sub> N <sub>2</sub>		(7.58 $\pm$ 0.15) $\times 10^3$	1.25 $\times 10^3$	0.0484

TABLE 1. Vibrational Energy Transfer Rates in CO-Additive Mixtures at 296°K.



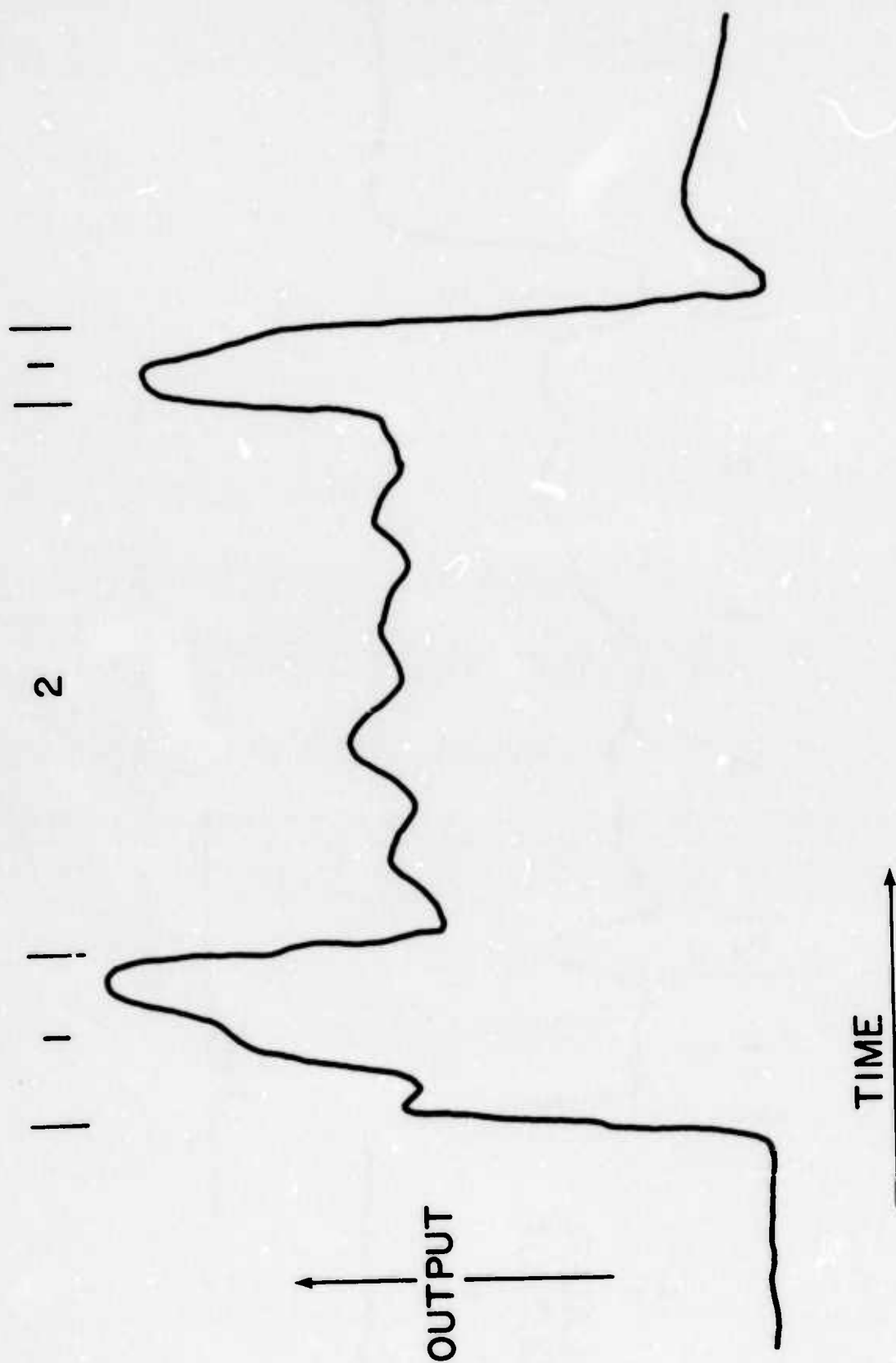


Fig. 1 - Effect of HF formed in the combustor on gasdynamic CO<sub>2</sub> laser output

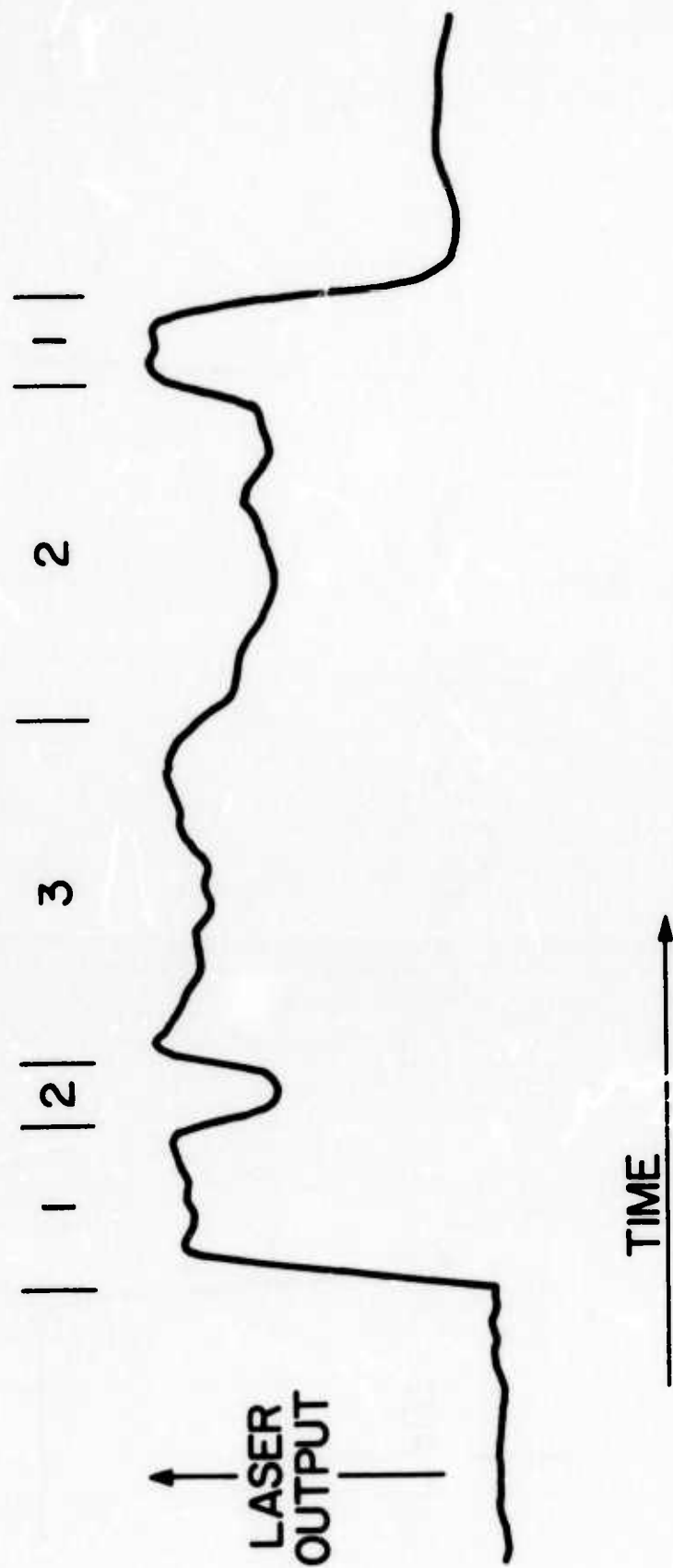


Fig. 2 - Chemical pumping of CO<sub>2</sub> gasdynamic laser

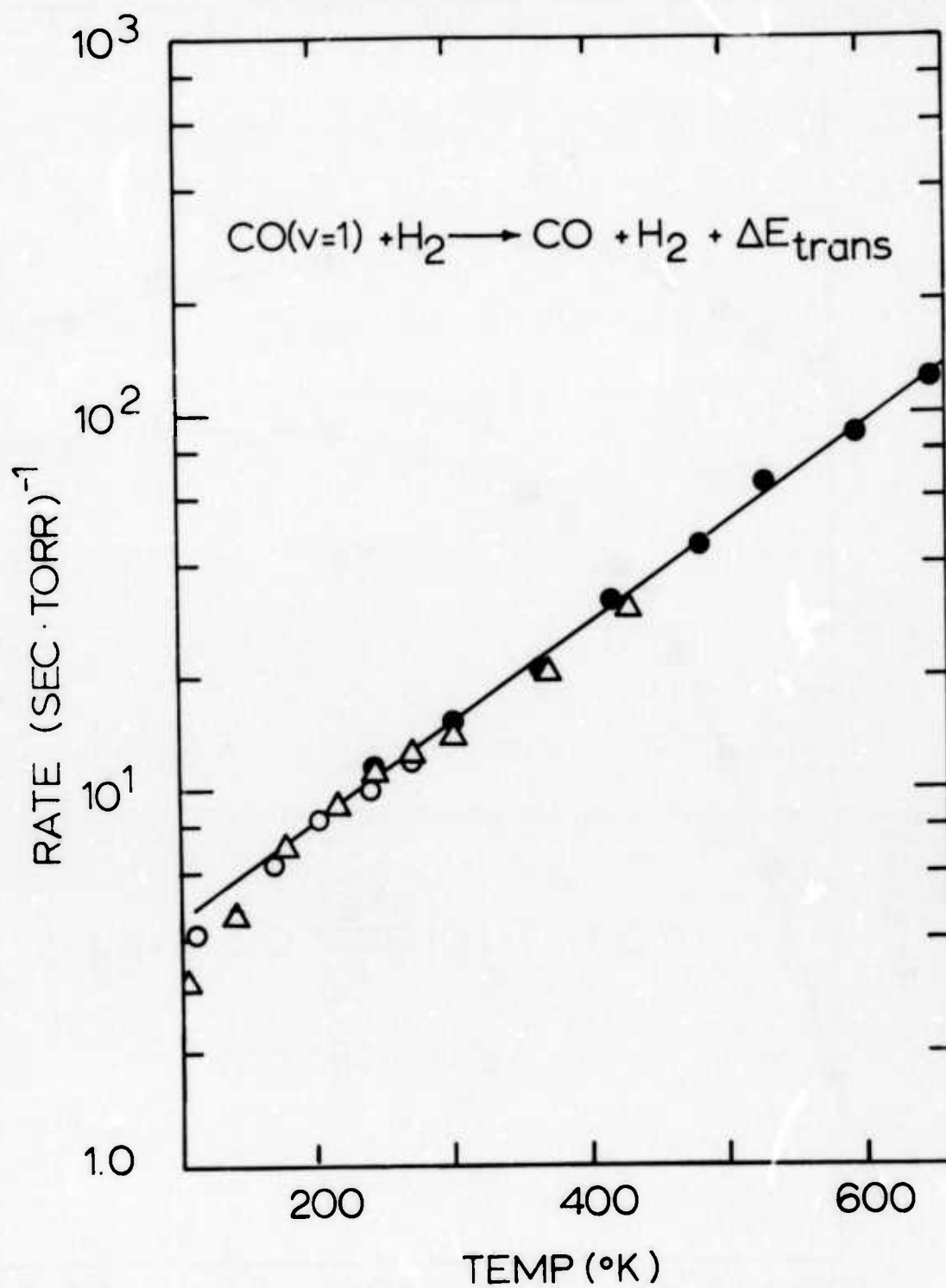


Fig. 3 - Temperature dependence of the rate of relaxation of  $\text{CO}(v=1)$  by  $\text{H}_2$ .

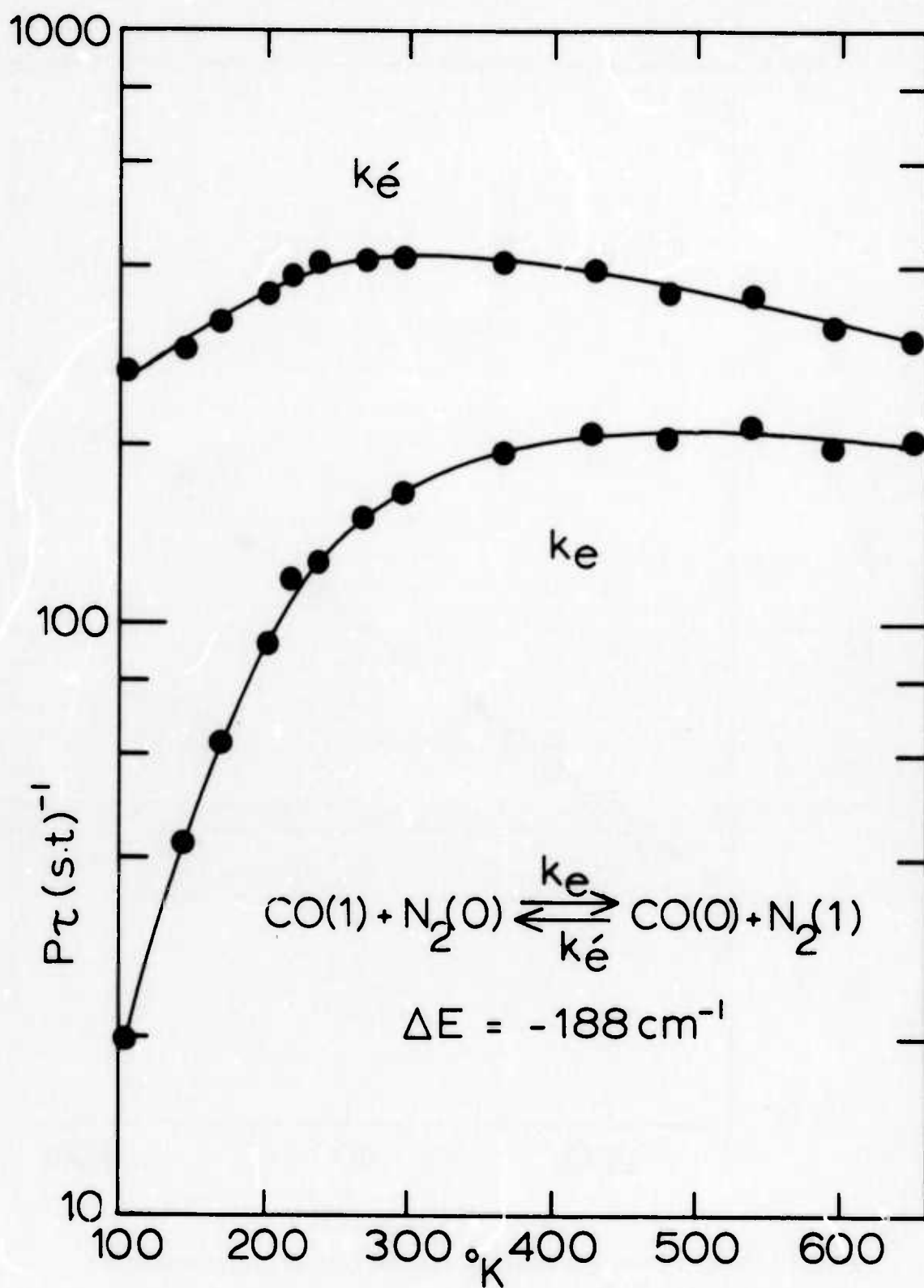


Fig. 4 - Temperature dependence of the relaxation times for V-V energy transfer from  $\text{CO}(v=1)$  to  $\text{N}_2$ .

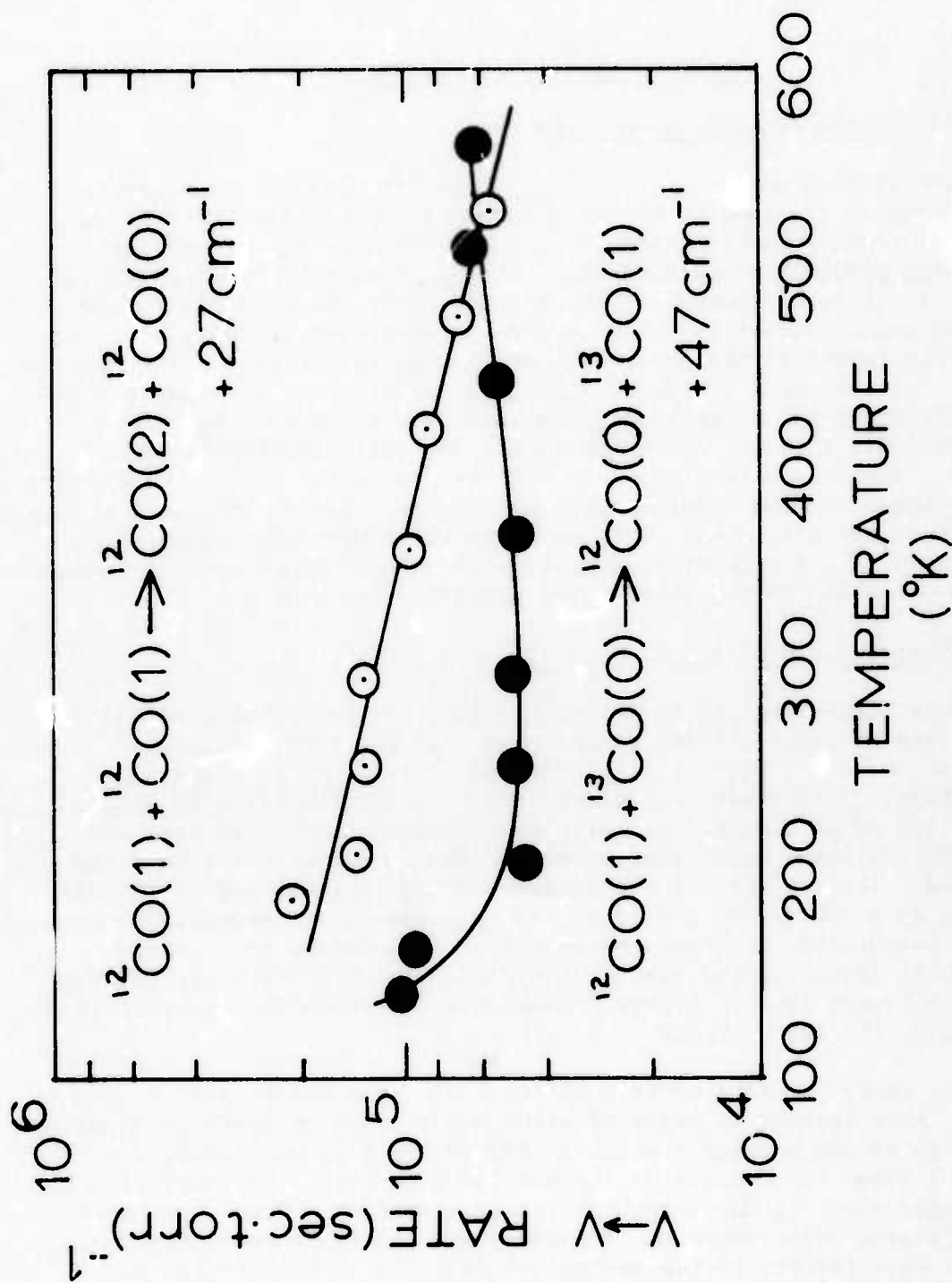


Fig. 5 - Temperature dependence of the rate of V-V pumping by CO(v=1) and the V-V energy transfer rate from  $^{12}\text{CO}(v=1)$  to  $^{13}\text{CO}$ .

## ELECTRICAL INFRARED LASERS

### 1. SHORT PULSE CO<sub>2</sub> MOLECULAR LASER

The work carried out under this section of the ARPA-NRL high energy laser program is aimed at the development of a reliable high-energy ( $\sim 30$  J) short-pulse ( $\sim 1$  nsec) CO<sub>2</sub> laser system. In the present reporting period the goals of this experiment have been surpassed in terms of the energy output of the system. Here the operation of the various components of the laser system is described in detail. Figure 6 shows the layout of the experiment which comprises a single short-pulse driver followed by a series of high gain amplifiers. For clarity, the description of the laser is divided into four sections. The first section deals with the operation of the low power short-pulse generation scheme. The second section deals with the operation of the preamplifiers. In the third section results taken on the operation of the large aperture amplifiers are discussed. Gain and gain uniformity measurements are described. The fourth section deals with results taken with the complete system operating in the short-pulse amplification mode.

#### (i) Short Pulse Oscillator

Efficient high-energy short-pulse CO<sub>2</sub> laser systems require reliable generation of input driving pulses with high pulse to background contrast, multi-rotational line spectral content and good spatial properties. With these considerations in mind, an oscillator system consisting of an acousto-optically mode-locked atmospheric pressure CO<sub>2</sub> laser followed by a pulse selection system has been designed and operated. The contrast of the isolated pulse is increased by passing it through a 100 cm CO<sub>2</sub> amplifier and then through a saturable absorber cell. Discussion of these components is included in this section since only after leaving them is the pulse suitable for amplification to the 30 joule level. Figure 7 shows the experimental layout of this section of the laser system.

The mode-locked oscillator is a helical pin, atmospheric pressure CO<sub>2</sub> laser. Mode locking is achieved using a 1.5 x 1.5 cm aperture Brewster-angled germanium modulator which is excited by a 20 MHz LiNbO<sub>3</sub> transducer. Figure 8 shows the details of the mode-locking unit. The modulator is positioned close to the output mirror of the laser. Careful control of the modulator drive power and frequency and the laser operating voltage and gas mix, results in the reliable production of mode-locked pulse trains with total energy  $\sim 70$  mJ. A single pulse is selected from the laser pulse train using a GaAs Pockels cell activated by a laser-



triggered spark gap. The GaAs Pockels cell has been successfully operated at its half-wave voltage. The system has also been designed to minimize reflection of the high voltage pulse applied to the Pockels cell since the reflected pulse can return at a later time and produce secondary switching. This is undesirable when the Pockels cell is used to select pulses for amplification in a high-gain amplifier chain.

The Pockels cell was constructed in the form of a 30 ohm parallel-plate transmission line (Fig. 9). After passing through the Pockels cell the high-voltage switching pulse is terminated in a 30 ohm resistive load. The electrical characteristics of the complete system was observed using time-domain reflectometry and in the final arrangement the voltage reflections at the various components were  $\leq 10\%$ . The switching effect of the Pockels cell is shown in Fig. 10. It can be seen that complete switching of the mode-locked pulse is achieved as a result of the operation of the crystal at its half wave voltage. The important characteristics of the Pockels cell switch are summarized below.

Pockels cell crystal	GaAs
Dimensions	8.6 x 8.6 x 50 mm
Passive extinction (measured by probing the crystal between crossed polarizers using a cw CO <sub>2</sub> laser)	$\sim 1400:1$
Optical loss	13%
Operating half-wave voltage	15 kV
Firing jitter	$\sim 2$ nsec
Number of shots taken	$\sim 10,000$ .

The above system routine selects single mode-locked pulses with energy  $\sim 3$  mJ. The intensity of leakage pulses is  $10^3$  lower than the main pulse.

Initial experiments on amplifying the switched-out pulse to a high energy showed that at the end of the amplifier chain, the leakage pulses contained as much energy as the main amplified pulse. Thus it was necessary to improve the initial contrast of the selected pulse. This was achieved by first passing the pulse through a 100 cm CO<sub>2</sub> amplifier and then through a saturable absorber cell. The amplifier increases the main pulse energy to  $\sim 50$  mJ. The effect of the saturable absorber is to transmit the high energy saturating pulse but absorb the low intensity leakage pulses. For the present laser system a 1 mm thick absorber cell containing 100-150 torr of SF<sub>6</sub> and  $\sim 600$ -650 torr helium has been used. Although the details of the operation of the cell have not yet been investigated it is estimated that the main pulse-background contrast is  $> 10^5$  after passing through this system. The SF<sub>6</sub> cell absorbs 40-50% of the main pulse energy and the energy entering the next section of the chain is typically  $\sim 20$  mJ.

Efficient nanosecond energy extraction from medium pressure (1-3 atm)  $\text{CO}_2$  amplifiers requires that the master oscillator should operate on as many  $\text{CO}_2$  rotational lines as possible. For this reason we have determined the spectral output of the short pulse oscillator. The mode-locked pulse train was directed through a 1 m spectrometer and the output was detected using a sensitive Ge:Cu detector. It is expected that the spectral content of the single switched-out pulse will not differ significantly from that of the complete pulse train. The laser spectrum is shown in Fig. 11. It is seen that the main energy output is on the P(16), P(18) and P(20) transitions of the  $00^0_1 - 10^0_0$  laser band. However measurable output also occurs on the other transitions between P(10) and P(26). Thus with this type of laser, multi-line operation is obtained without external assistance. This is a desirable effect in terms of maximizing the energy extracted from the amplifiers and also helps to prevent the amplified laser pulse from lengthening since in a saturated amplifier (using single line input) rotational repumping of the tail of the pulse can occur, thereby increasing the pulse halfwidth.

The properties of this section of the laser system are summarized in the following table:

#### SINGLE PULSE GENERATOR

Method of production	Acousto-optically mode-locked laser and single pulse selection
Pulse selection system	GaAs Pockels cell with stacked Ge plate polarizers
Mode structure	$\text{TEM}_{00}$
Single pulse energy	$\sim 20 \text{ mJ}$
Pulse to background contrast	$\geq 10^5$
Pulse spectrum	Multi-line (P(10) - P(26) of $00^0_1 - 10^0_0$ transition)
Pulse width	$\sim 1.2 \text{ nsec.}$

#### (ii) Small Signal Amplifiers (Pre-amps)

In the work carried out during this reporting period three of these amplifiers were in use. These units are of the solid electrode type employing UV preionization from line discharges. Each amplifier had a volume of  $3 \times 3 \times 50 \text{ cm}^3$  and was excited using a Marx generator (0.05  $\mu\text{F}$  erected capacitance capable of 80 kV operation). We have investigated the gain characteristics of these amplifiers over a wide range of gas mixtures ( $\text{He}:\text{CO}_2:\text{N}_2$ ) and were able to sustain glow discharges in mixtures containing up to 35%  $\text{CO}_2$ , achieving gain coefficients up to  $0.0326 \text{ cm}^{-1}$ . The gain measurements were taken using a stabilized cw  $\text{CO}_2$  laser which was tuned to operate on line

center of the  $00^0_1 - 10^0_0$  P(20) transition. The measured gains are shown in the following table.

%He	%CO <sub>2</sub>	%N <sub>2</sub>	CHARGING VOLTAGE GLOW RANGE (kV)	MAXIMUM GAIN COEF. (cm <sup>-1</sup> )
60	25	15	28-38	0.0249
55	25	20	33-39	0.0269
50	25	25	39-44	0.0301
70	30	0	21-26	0.0089
65	30	5	23-30	0.0190
60	30	10	24-32	0.0210
55	30	15	28-35	0.0250
50	30	20	33-41	0.0287
45	30	25	37-42	0.0325
45	35	20	34-39	0.0309

In normal operation these amplifiers were operated using a 60:25:15 laser mix and a charging voltage ~37 kV (~74 kV Marx erected voltage). These values were chosen as the best compromise between high gain operation and high reliability.

### (iii) Large Aperture Amplifiers

The final amplifiers of the short pulse laser system consist of two Lumonics series 600 amplifiers stages followed by an electron beam controlled amplifier which was supplied by Maxwell Labs. The clear aperture of each amplifier is ~ 10 cm diameter and a X 2.7 off-axis Cassegrain telescope is used to increase the laser beam diameter out of the 3 x 3 x 50 amplifiers to match the cross-sectional area of the final stages. The gain of the Lumonics amplifiers was checked using a cw CO<sub>2</sub> probe laser beam. A peak gain of ~ 0.038 cm<sup>-1</sup> was measured for a He:CO<sub>2</sub>:N<sub>2</sub> mix of 60%:30%:10% with an energy loading of 300 J/l. The uniformity of gain was checked at a few points across the aperture of the device. The gain variation for the points measured was +3%.

Generally speaking the Lumonics amplifiers have worked quite reliably. Four major problems were encountered during their initial use. These are listed below along with the remedies used.

#### (a) Excessive Jitter of Gain Pulse

The problem here was due to the method employed in firing the preionizer. In these amplifiers, preionization is achieved by firing a series of small spark gaps which are physically positioned behind a screen anode. For best operation these gaps should be fired ~ 0.5 - 2.0 μs before the application of the main discharge. In the original equipment the firing delay for the main Marx was achieved by use of pressurized spark gaps. A single trigger pulse was used to fire two

spark gaps; one for the gap in the pulse line to the preionizer gaps and the other in the main discharge line. The desired delay was achieved by operating the main discharge spark gap well above its self-breakdown pressure. The jitter introduced by this firing method was found to be excessive and resulted in large shot-to-shot peak gain variation. This problem was solved by triggering the main Marx using a pulse derived from the preionizer discharge. The necessary delay is achieved by use of a high-voltage delay line.

(b) Unreliable Triggering of Main Marx

Triggering of the main Marx spark gap is achieved using a standard automobile spark plug. The problems encountered were due to erosion of the trigger pin of the spark plug. This was solved by replacing the pin with a tungsten rod. This rod shows no sign of erosion and has worked reliably for many months.

(c) Cathode Support Structure Failure

In the Lumonics amplifiers the cathode consists of a solid metal block held in a Bakelite support structure. Due to the weakness of the support, the cathode gradually bowed in towards the anode. This reduced the distance between the laser electrodes and caused the E/N in the laser gas (at maximum charge voltage) to exceed that required for maintaining glow discharges. Arcing occurred when maximum charging voltages were used. This problem was rectified by Lumonics who sent attachments to improve the strength of the cathode supports.

(d) Capacitor Failure

After a few months use one of the laser Marx capacitors became faulty. Lumonics replaced this under warranty.

The final amplifier stage in the laser system is a 10 cm aperture x 100 cm long electron beam controlled device. This equipment was delivered, installed and tested during the present reporting period. Preliminary gain measurements were taken on the amplifier at operating pressures of 800 torr and 1550 torr using the experimental set up shown in Fig. 12. A dual beam oscilloscope was used to display the amplifier gain pulses and the low level probe pulse on each firing of the device.

The uniformity of gain across the aperture of the device has been investigated. Measurements were taken along diameters midway between the electrodes (vertical gain scan) and from anode to cathode (horizontal gain scan). The results are shown in Fig. 13. Gain variations of  $\pm 15\%$  were observed and on the horizontal scan there was a noticeable drop-off of gain towards the amplifier cathode. This effect has also been observed in similar devices of other manufacture, and has been



attributed to a reduction of E/N in the vicinity of the cathode due to the field shaping effects associated with the proximity of the laser chamber walls. Solution of this problem would involve the fitting of a larger laser chamber which is not presently planned. However, such a modification would be necessary to ensure maximum laser beam uniformity out of the amplifier.

Various laser gas mixtures were tested to determine which gave the highest gain. The best mix tested was He:N<sub>2</sub>:CO<sub>2</sub> (3:4:1) which correlates with results taken in other laboratories using similar devices. The amplifier has been operated at pressures up to 1550 torr. At the highest operating pressure the dependence of optical gain on energy input to the gas has been investigated. Also investigated was the effect of using different rates of energy input. The results of those experiments are shown in Fig. 14. The upper limit of the gain measurements was set by the point at which the amplifier self oscillated. The best gain achieved was  $\sim 0.05 \text{ cm}^{-1}$  for an energy input to the gas  $\sim 200 \text{ J l}^{-1}$ . It can be seen from the curves of Fig. 9 that the achieved gain (for high energy input) is reasonably insensitive to the rate of energy input to the gas. The difference between the results for the different energy input rates is well within the experimental error. This information is important for the design of fixed parameter e-beam controlled amplifiers. The Maxwell machine was purposefully designed to be versatile so that investigations of this nature could be carried out. The results shown were taken with the laser sustainer bank charged to  $\sim 74 \text{ kV}$ .

Higher pressure operation of the amplifier is desirable since it decreases the rotational relaxation time in the gas and thus pulse broadening due to rotational repumping can be avoided. The present e-beam machine is however not well suited to high pressure ( $> 3 \text{ atm}$ ) operation, since the sustainer bank is limited to 75 kV charge voltage. Thus it is not possible to reach the E/N required for optimum pumping of the CO<sub>2</sub> and N<sub>2</sub> vibrational levels at these pressures. The machine does however operate with high gain at pressures up to  $\sim 2$  atmospheres. (See Fig. 14).

#### (iv) Pulse Amplification Experiments

Pulse amplification experiments were carried out towards the latter part of the reporting period. The laser chain was set up as shown in Fig. 6. The main problems encountered were due to self-oscillation of the amplifier chain (total small signal gain  $\sim 70 \text{ dB}$ ). This problem was traced to scatter from amplifier windows and from defective coatings in the beam expander. All the amplifier NaCl windows were replaced and new coatings were applied to the beam expander optics. In addition it was necessary to cover all laser box surfaces close to the laser axis with fiberglass. Fiberglass is strongly absorbing at  $10.6 \mu\text{m}$  and prevents reflections from the lucite boxes and aluminum

window holders. After these modifications it was found that self-oscillation of the chain did not occur. This was determined by placing a calorimeter at the output of the amplifier chain and firing all the system components except the oscillator.

Calorimeters were placed at various points in the amplifier chain to monitor the pulse energy at various points. This was achieved by directing the reflections from the various amplifier windows into the calorimeters. A calibrated photon drag detector was used to monitor the pulse energy out of the mode locked pulse-selection system. These various monitors are shown on Fig. 6. Oscilloscope traces of the laser pulse at various points in the chain were also taken to observe changes in the pulse shape as it progressed down the amplifier.

During initial operation the maximum amplified laser pulse energy was measured to be  $\sim 50$  J. This output was achieved for an energy input of  $\sim 10$  J into the e-beam amplifier stage. There was some variation in the output energy and this was traced to triggering jitter in the oscillator circuit. Oscilloscope traces of the laser pulse were taken at various points in the chain and typical recordings are shown in Fig. 15. The effects of amplifier saturation are clearly seen as causing the broadening of the laser pulse as it progresses down the chain. The biggest effect is seen at the output of the electron beam amplifier as this amplifier is being heavily saturated.

Figure 16 shows a set of results taken of energy in vs energy out of the electron beam amplifier. Since the spatial uniformity of the input laser was poor, it is not possible to calculate a meaningful number for the saturation parameters of the amplifier. These results were taken at 2 atmospheres and demonstrate the possibility of obtaining high pulse energy from the system. Calculation shows that the stored energy in the volume of the e-beam, swept by the laser pulse, is in the region of 80 - 90 J. The amplified pulse energy of 50 J is not inconsistent with these calculations. With higher pressure operation of the e-beam and using higher pulse energy from the Lumonics amplifier, it should be possible to obtain an output pulse energy  $\sim 100$  J.

#### CONCLUSIONS

The high power, short pulse  $\text{CO}_2$  laser has been completely assembled and operated at energies up to 50 joules. At this level of operation no damage problems were encountered in any part of the system. The main problem with the system was one of synchronization. At present the trigger jitter of all the components of the amplifier chain is being improved. Another 3 x 3 x 50 cm amplifier will be added.

In the experiments to date, the energy out of the oscillator switch-out system was limited to  $\sim 3$  mJ. The helical laser tube is being replaced



by a solid electrode double discharge device. It is expected then that oscillator pulse energies  $\sim 10$  mJ will be available. Future experiments will concentrate on obtaining the maximum energy out of the complete system. The electron beam amplifier will be operated at 3 atmospheres. It is expected that an output pulse energy  $\sim 100$  J will be attained. Measurement of the saturation energy of this amplifier will be carried out.

## 2. ELECTRIC DISCHARGE GASDYNAMIC LASER, EDGDL

A subatmospheric plenum EDGDL has been designed and fabricated in order to study the  $D_2$ -HCl transfer laser system. The system has been designed such that it can be easily modified to operate in different flow regimes (subsonic or supersonic) and with different types of electrical excitation (RF or DC). The initial experiments will be performed with a subsonic plenum in which  $D_2$  diluted in Ar is vibrationally excited by an electric discharge and then expanded through an array of nozzles whose area ratio,  $A/A^* = 7$ . HCl is injected part way through the supersonic portion of the nozzles. This mixing scheme was chosen to promote mixing of the heavy molecular weight HCl into the primary  $D_2$ -Ar flow. The system can then be observed through the Brewster angle windows which extend  $4\frac{1}{2}$  inches downstream of the nozzle exit plane. A picture of the unassembled system is shown in Figure 17 and a schematic is shown in Fig. 18.

The vibrationally excited  $D_2$  produced in the plenum transfers vibrational energy to HCl. As a result of the gasdynamic cooling the HCl should undergo anharmonic V-V pumping thus creating a partial inversion of the vibrational levels of HCl. The use of the  $D_2$  transfer to HCl will prevent the direct heating of the HCl by the electric discharge.

Initially, HCl fluorescence will be monitored to optimize mixing and demonstrate the transfer of vibrational energy from  $D_2$  to HCl. These experiments will be followed by the construction of a high Q cavity to investigate the lasing potential of this system.

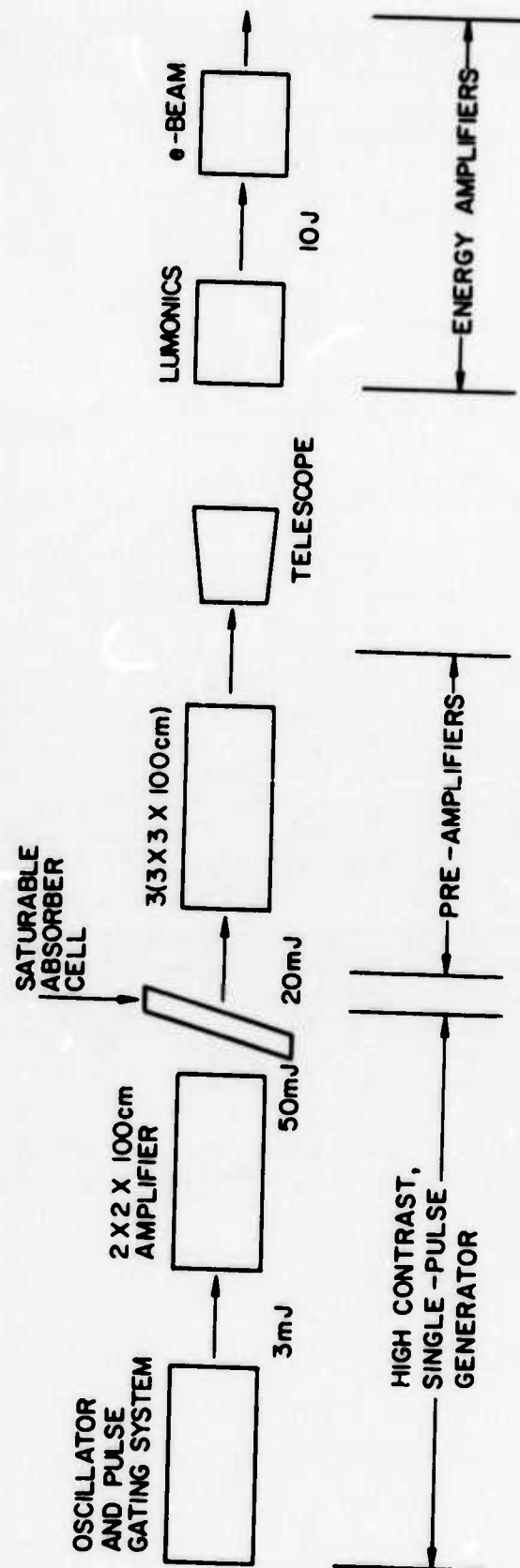


Fig. 6 - Diagram of layout of complete laser system.

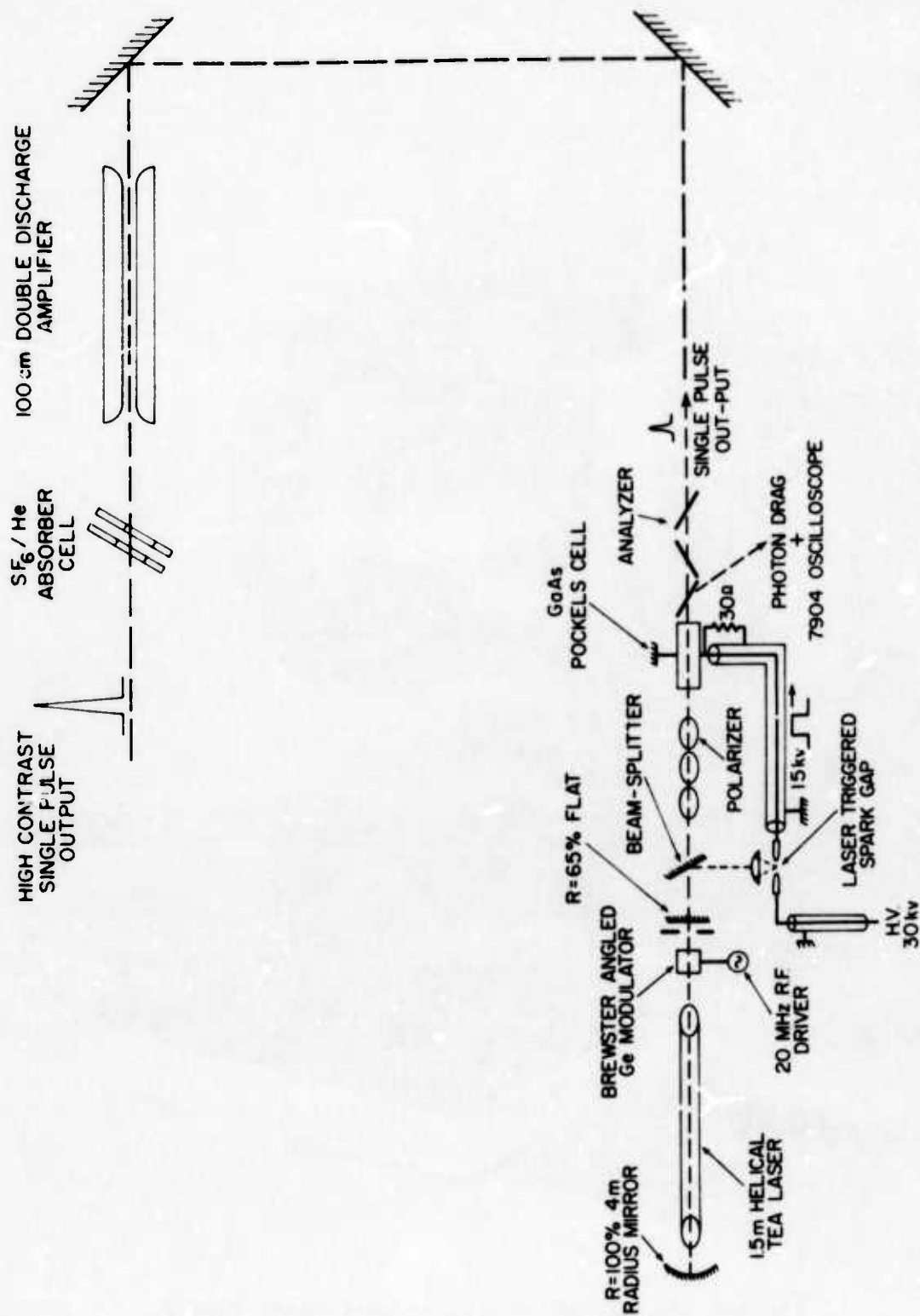


Fig. 7 - Detailed diagram of high contrast single pulse generator.

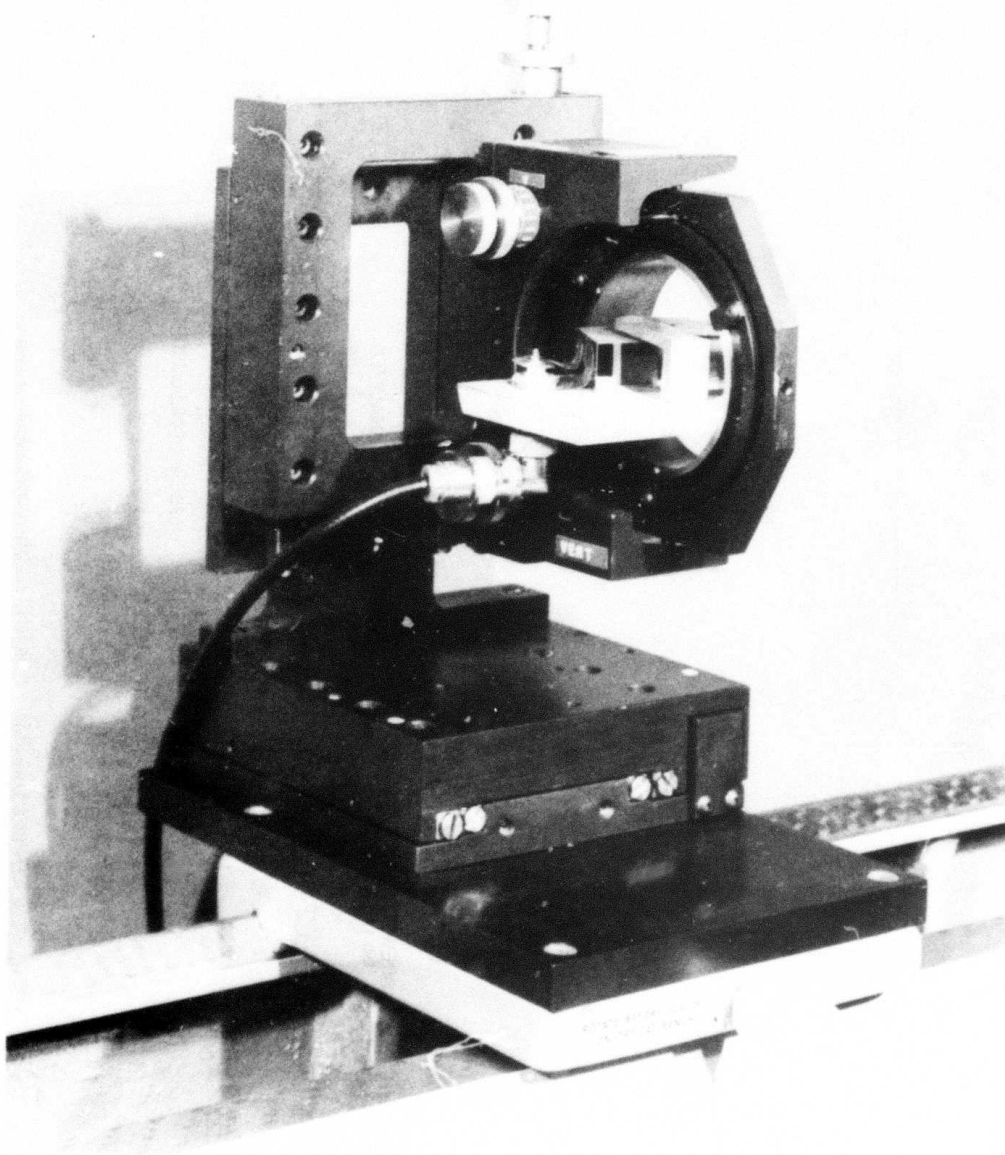


Fig. 8 - Photograph of acousto-optic mode locker.

Reproduced from  
best available copy.



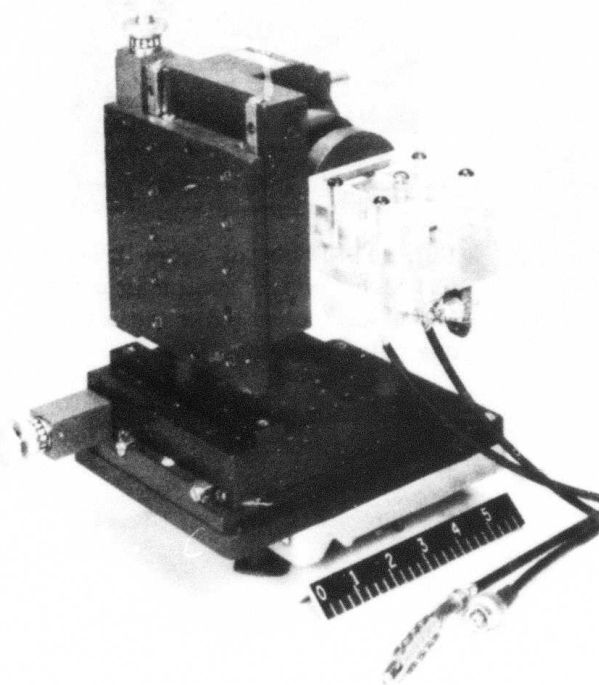
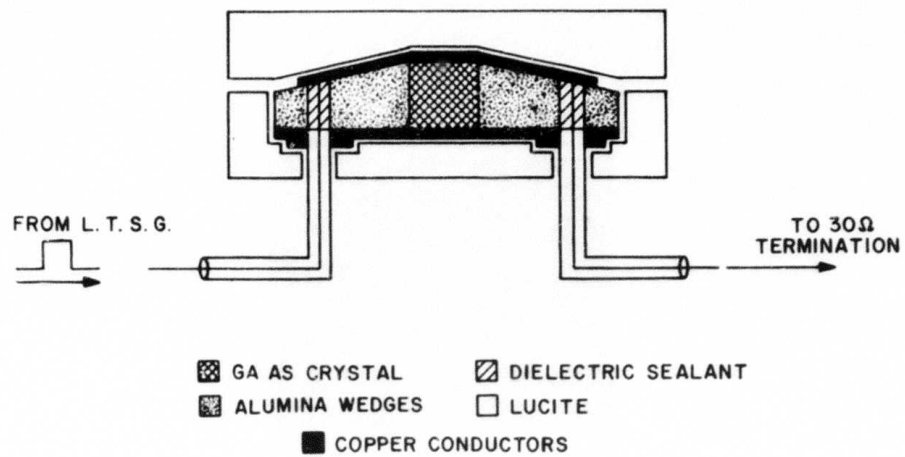


Fig. 9 - Photograph of Pockels cell and design diagram

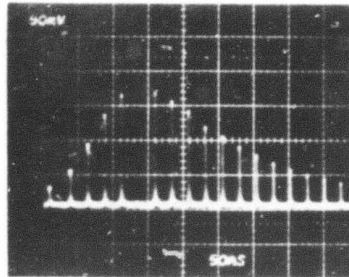
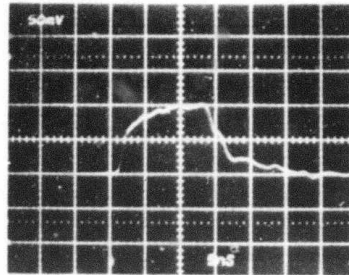


Fig. 10 - Photo of scope traces  
 (1) high voltage switching pulse  
 (2) mode locked pulse train with  
 one pulse missing.



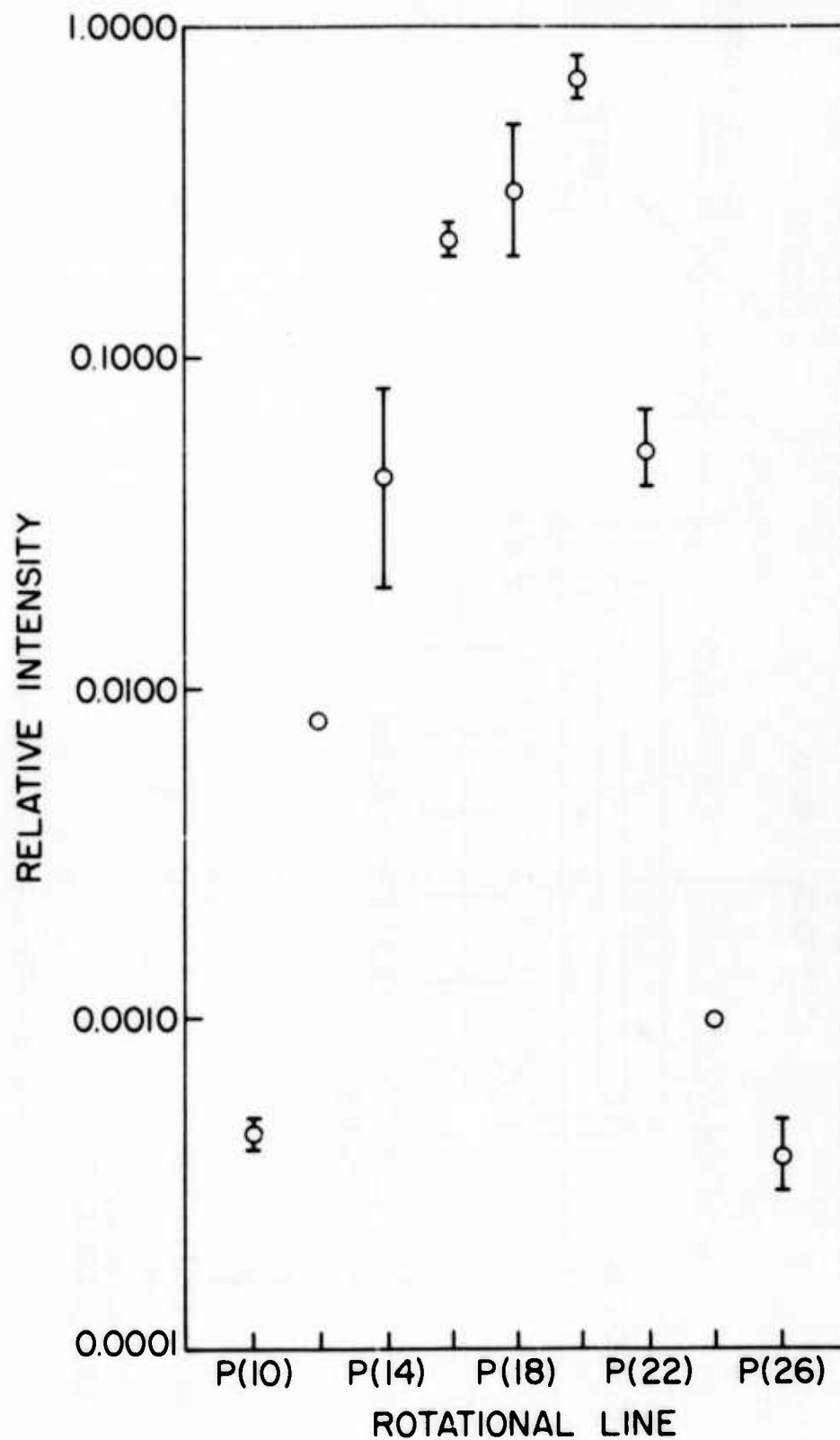


Fig. 11 - Oscillator spectrum.

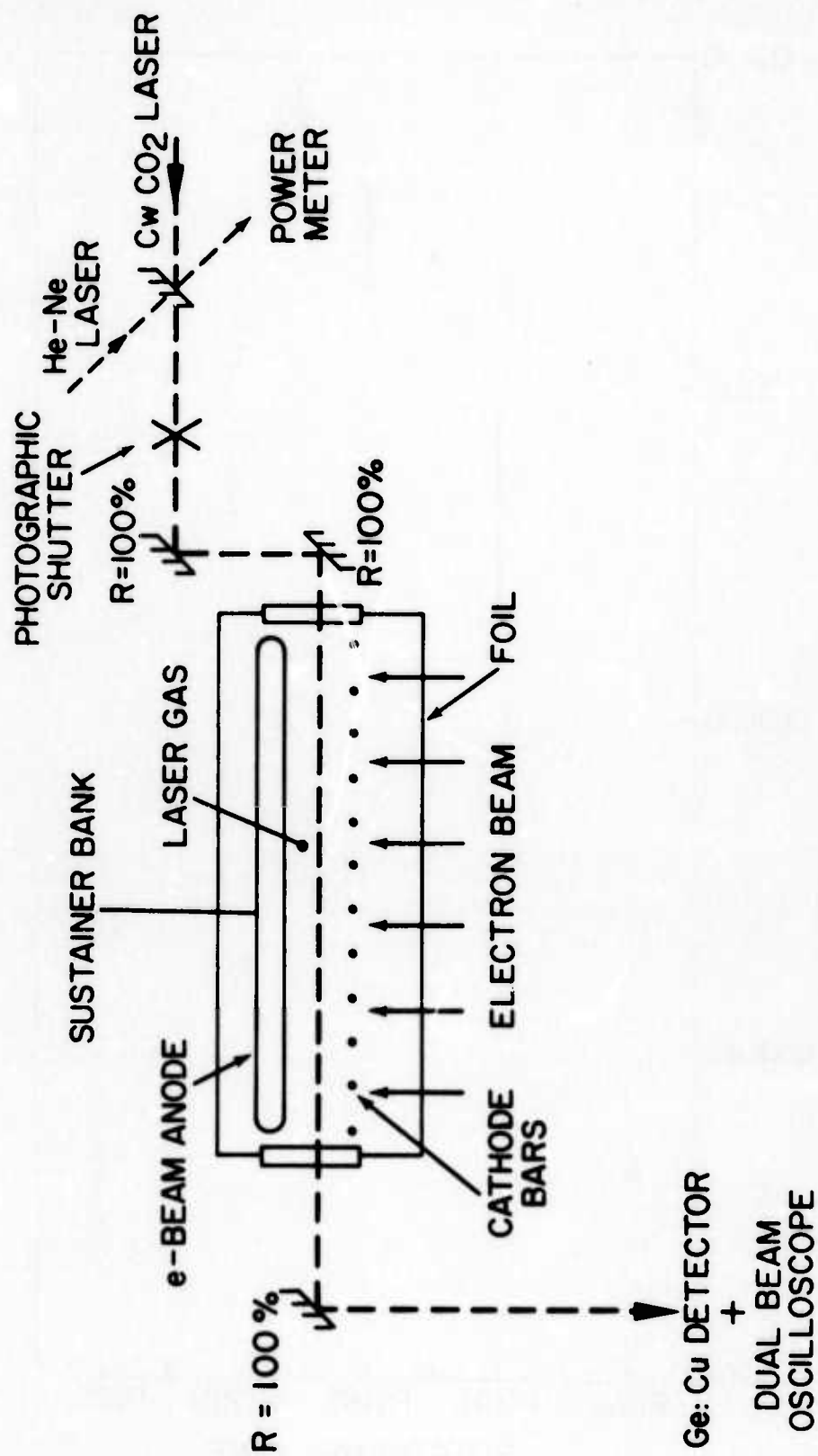


Fig. 12 - e-Beam gain measurement set-up and typical result.

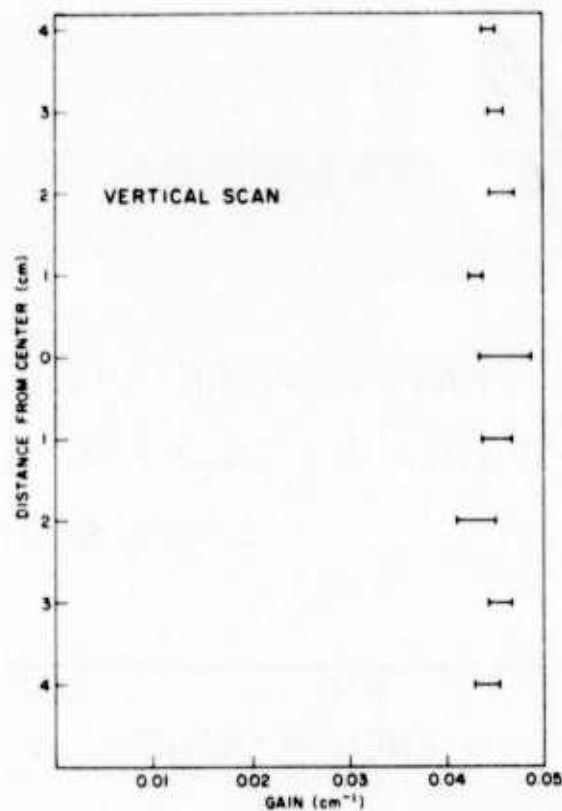
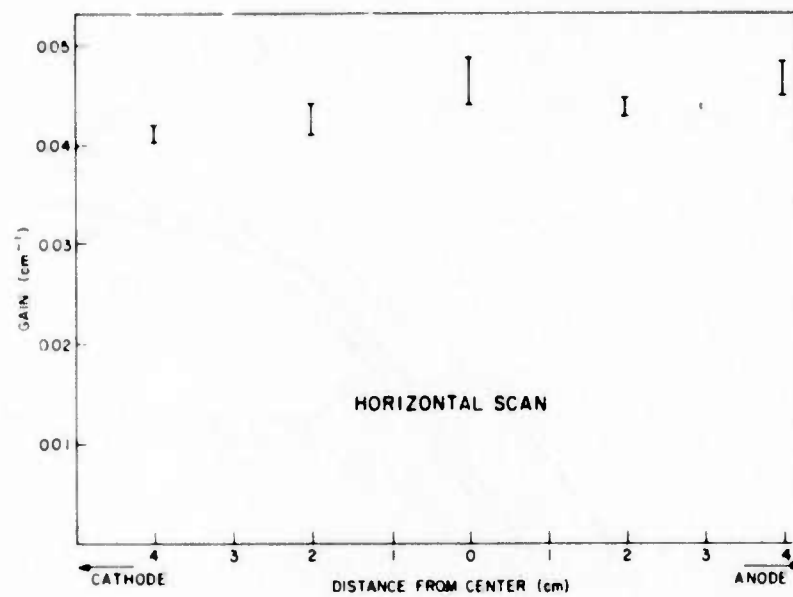


Fig. 13 - Gain uniformity measurements on e-beam.

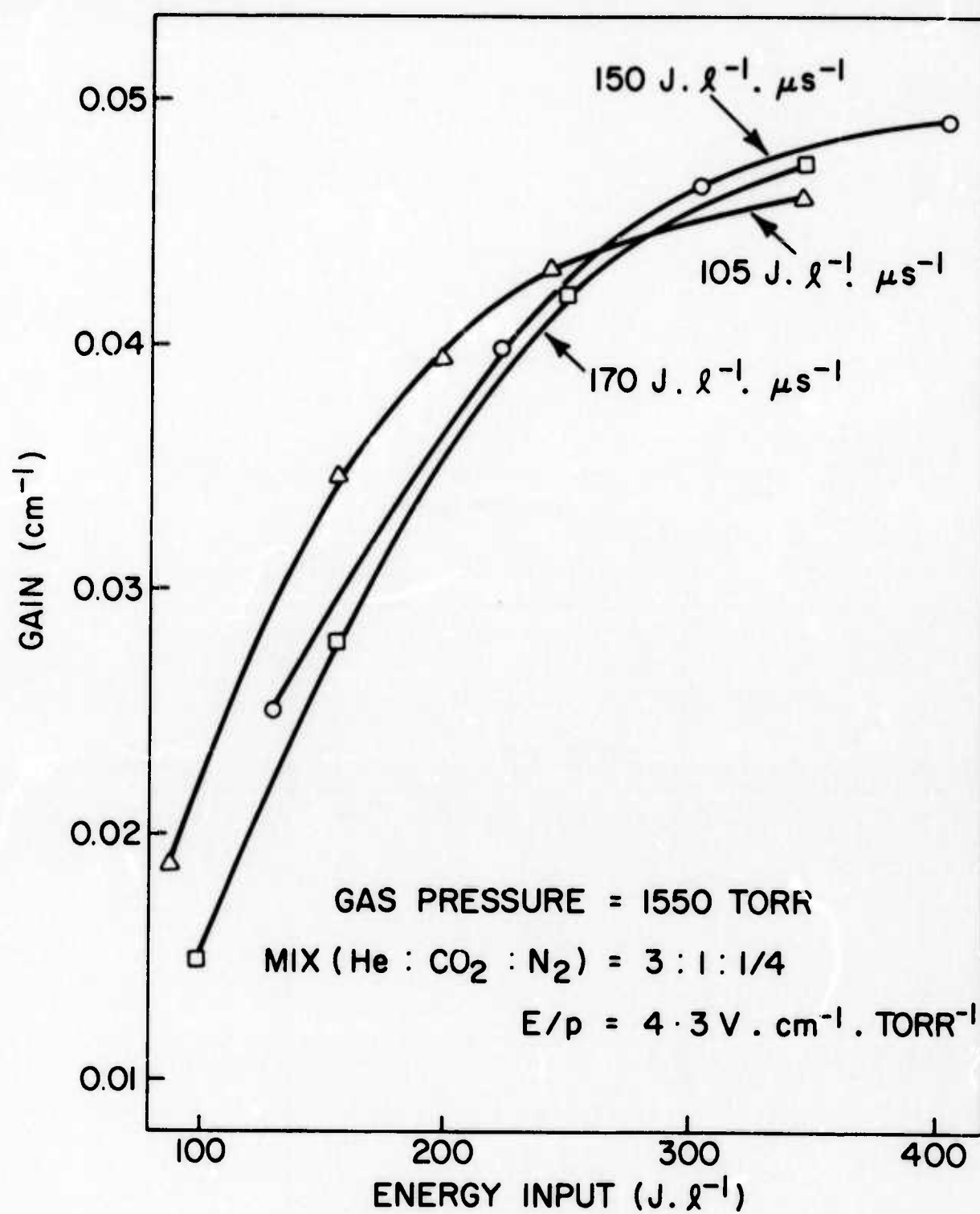
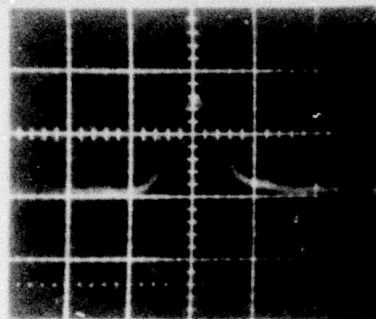
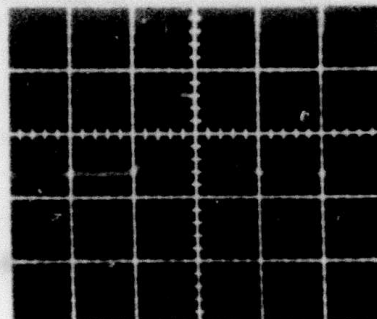


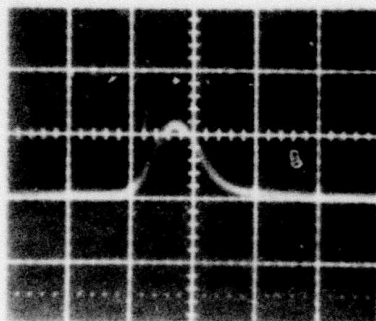
Fig. 14 - Gain vs energy input for e-beam at 2 atm.



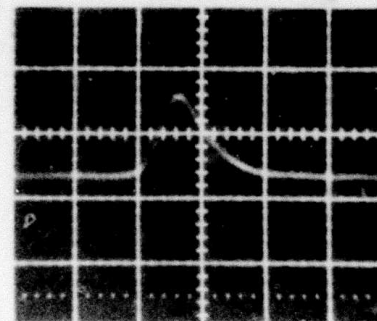
a. OSCILLATOR



b. SMALL SIGNAL AMPLIFIERS



c. LUMONICS AMPLIFIERS



d. ELECTRON BEAM AMPLIFIER

**Fig. 15 - Oscilloscope traces of nanosecond pulse at various stages of amplification.**

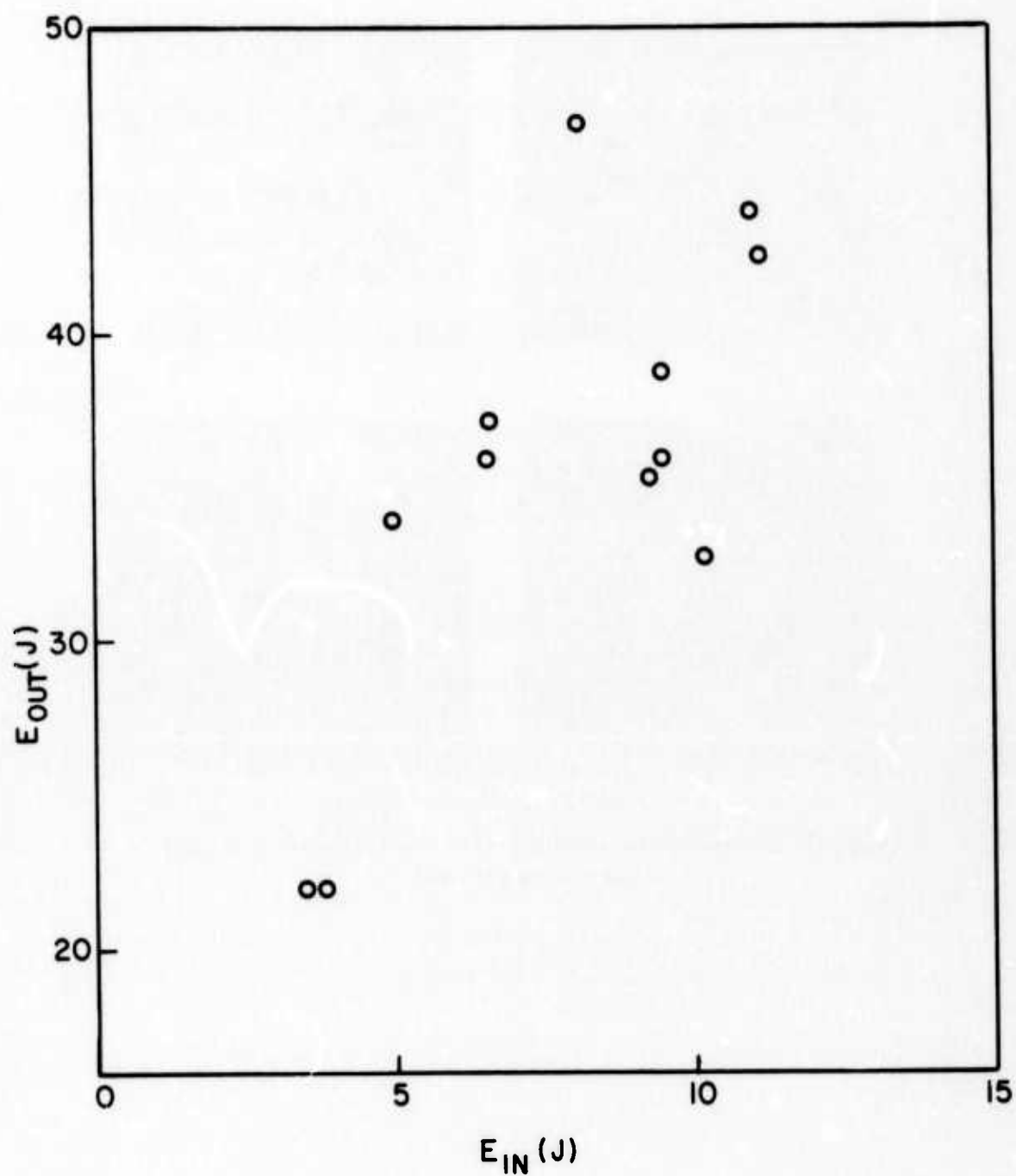


Fig. 16 - Results of pulse amplification with e-beam amplifier .



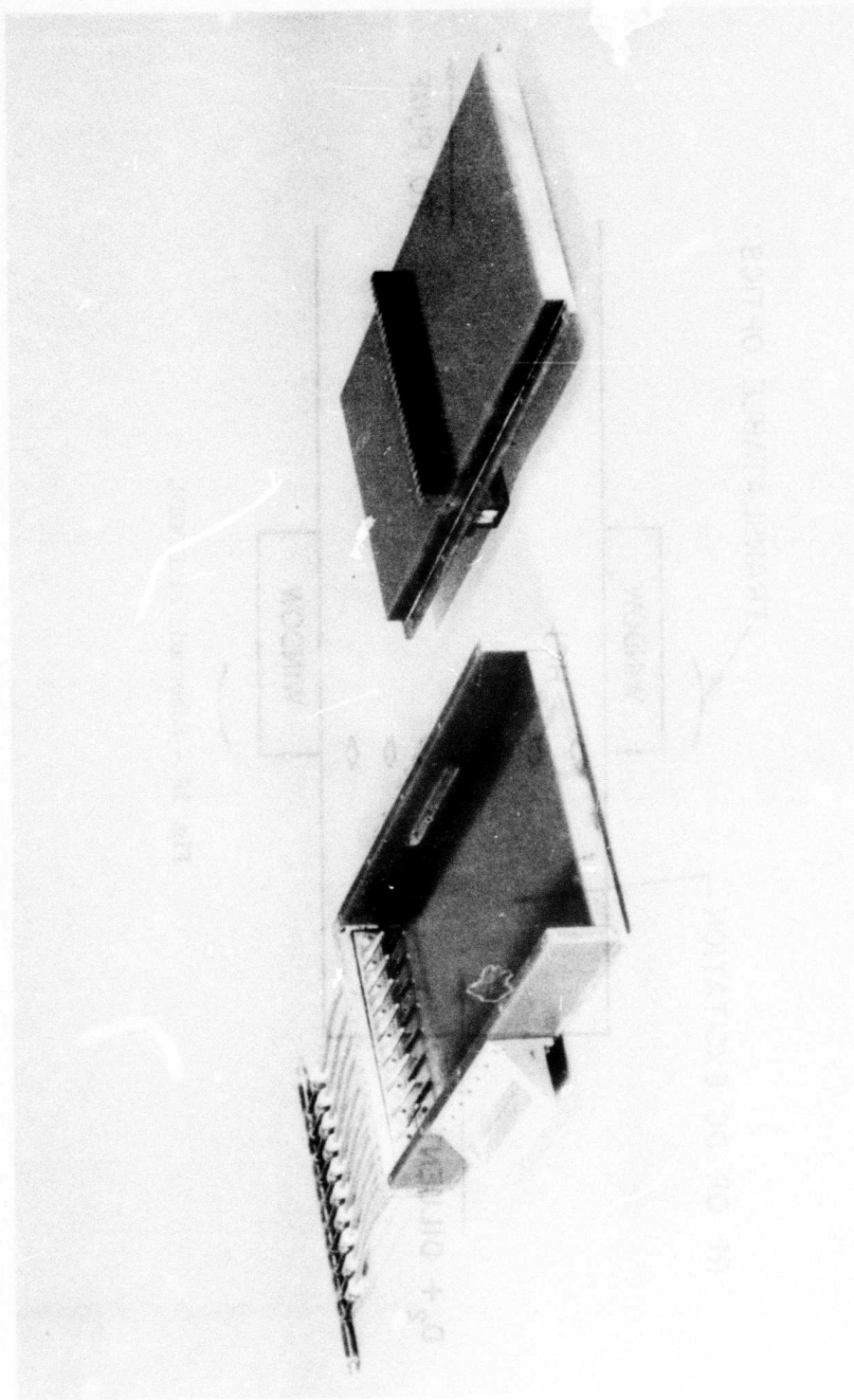


Fig. 17 - EDGDL Apparatus

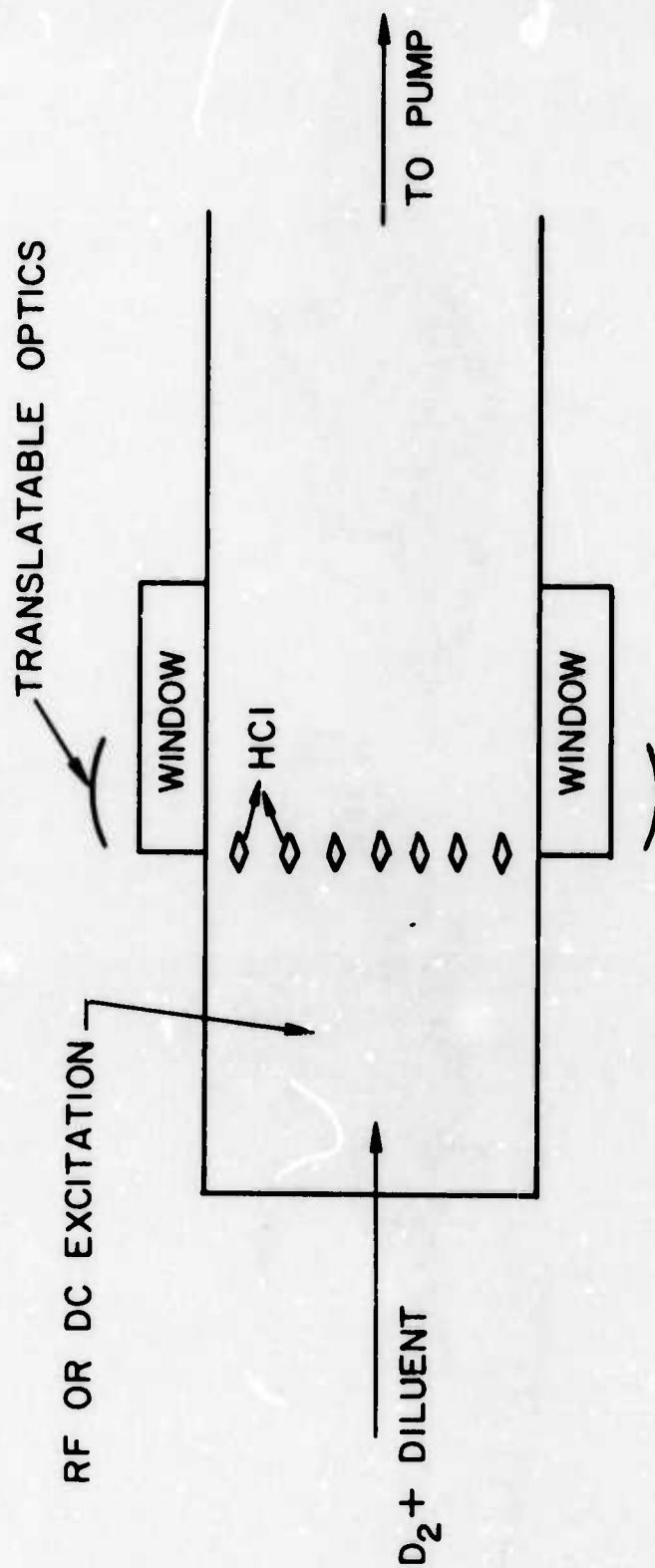
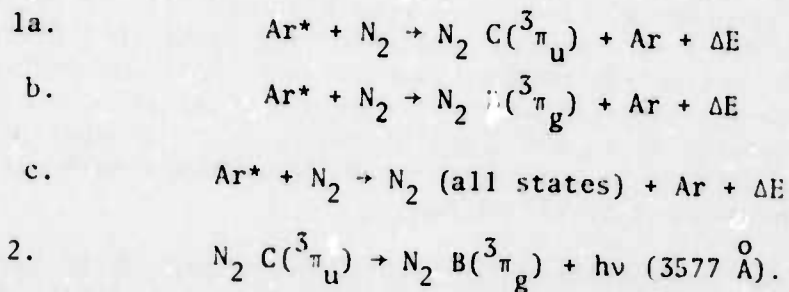


Fig. 18 - Schematic of EDGDL

## ELECTRONIC STATE LASERS

### 1. ELECTRON BEAM INITIATED VISIBLE TRANSITION LASERS

High energy electrons efficiently produce rare gas metastable species,  $R^*$ . Thus, if energy transfer from  $R^*$  to a suitable acceptor molecule is kinetically favored, visible or near uv electronic state lasing transitions may be efficiently pumped by this process. This report evaluates energy transfer from metastable argon,  $Ar^*$ , to  $N_2$  as a means of creating lasing in  $N_2$ , by the following mechanisms.



The parameters of interest are the ratio of the rate constant for reaction 1a to that for reaction 1c and the ratio for populating the upper and lower laser levels  $k_{1a}/k_{1b}$ .

Considerations of resonant energy transfer suggest that the argon metastables will preferentially populate the  $N_2 C$  state since its energy level is only  $3000 \text{ cm}^{-1}$  below that of the metastable. The  $N_2 B$  state by comparison lies  $33,000 \text{ cm}^{-1}$  below the argon metastable.

Thus the  $Ar-N_2$  system should form the basis of an efficient laser if resonant electronic energy transfer is the dominant process in this system for excitation of nitrogen.

The  $Ar-N_2$  system has been studied by several groups. Prince et al<sup>(2)</sup> reported the occurrence of step 1a but did not report any direct

1. D.C. Lorents and R.E. Olson, Stanford Research Institute Report PYU-2018 (December 1972).
2. J.F. Prince, C.B. Collins and W.W. Robertson, J. Chem. Phys. 40, 2619 (1964).

production of the  $N_2(B)$  state via step 1b, although this state was observed in emission in experiments with Ar- $N_2O$  mixtures. On the other hand, Setser et al<sup>(3)</sup>, found that Ar\* yielded six times as many  $N_2(B)$  as  $N_2(C)$  and Gutcheck and Zipf<sup>(4)</sup> measured  $k_{1a}$  to be only 0.4% of  $k_{1c}$ . Recently, Nelson et al<sup>(5)</sup> have carried out experiments in which long (up to 20  $\mu$ sec) superfluorescent C-B pulses were observed after excitation of Ar- $N_2$  mixtures, containing a trace of HF, in an electron beam-sustainer device. The latter experiment suggests that step 1a is the dominant energy transfer pathway.

The present research program is intended to clarify the applicability of resonant energy transfer to systems such as Ar\*- $N_2$  and to explore various possibilities for increasing the efficiency of the 3577 Å band  $N_2$  laser.

The NRL 50 ns high-power electron beam generator was used to excite Ar- $N_2$  mixtures. The mixtures were contained in a laser cell fitted with a 15 cm x 1 cm electron beam entrance window whose optical axis was transverse to the electron beam. The cell was designed to allow operating temperatures up to 600°C and pressures up to 40 atm. The high temperature feature is necessary for planned future work with involatile compounds such as TlI or HgCl<sub>2</sub>.

The following data were obtained for each electron beam shot: integrated optical emission intensities on a 1 m Jarrell-Ash spectrometer, electron beam current waveform, and side and axial time dependent emission intensities. The three oscillograms obtained on each shot were synchronized by a fiducial time marker circuit whose accuracy was  $\pm 2$  ns.

Laser emission was observed over the range 250 - 5300 torr in a 19:1 Ar: $N_2$  mixture. The laser emission was characterized by a FWHM 25 ns pulse which was considerably narrower than the spontaneous emission pulse. The (0-0) vibrational band which was a strong emitter in fluorescence was absent in the laser output. The (0-1) band at 3577 Å and occasionally the 0-2 band at 3805 Å made up the laser spectrum. A cavity was necessary for laser emission.

At low pressure the spontaneous emission peaked after the end of the current pulse and was followed by the laser pulse. Higher pressure shifted the observed fluorescence and laser emission forward in time.

3. D.W. Setser, D.H. Stedman and J.A. Coxon, J. Chem. Phys. 53, 1004 (1970).
4. R.A. Gutcheck and E.C. Zipf, Bull. Amer. Phys. Soc. 17, 395 (1972).
5. L.Y. Nelson, G.J. Mullaney and S.R. Byron, Appl. Phys. Lett. 22, 79 (1973).

A computer code was used to model the results. Whereas a quantitative understanding of the laser mechanism awaits completion of the theoretical model, the following features are apparent.  $\text{Ar}^*$  rather than  $\text{Ar}_2^*$  is responsible for pumping the  $\text{N}_2(\text{C})$  state. Only at pressures higher than those encountered in this study will the termolecular formation of  $\text{Ar}_2^*$  result in energy transfer from  $\text{Ar}_2^*$  being dominant rather than from  $\text{Ar}^*$  to  $\text{N}_2$ . The observation of laser emission is inconsistent with the reported value<sup>(2)</sup> of six times as many  $\text{N}_2(\text{B})$  as  $\text{N}_2(\text{C})$  coming from  $\text{Ar}^* - \text{N}_2$  collisions. Furthermore the fluorescence measurements suggest that a yield of  $\text{N}_2(\text{C})$  of 0.4% cited in reference (3) is much too low.

It is expected that the  $\text{Ar}-\text{N}_2$  project will be completed in the near future. At that time research will begin on energy transfer from excited rare gases to metal halides and metal atoms.

## 2. DOUBLE-PULSE EXCITATION TECHNIQUES

The concept of double-pulse excitation is to produce laser action in gaseous species which are not normally stable at ambient or near ambient conditions. The first pulse is intended for optimum production of the desired species and the second pulse designed for optimum excitation.

An RF-DC double-pulse system has been assembled with the following characteristics.

RF Supply: 20 MHz, pulsewidth 5 microseconds to CW. Repetition rate to 1 KHz. Coil current to 12.5 amps RMS, depending on gas fill.

DC Supply: Pulse width 5 microseconds to 130 microseconds. Repetition rate to 1 KHz. Current to 4 amps, depending on gas fill.

Pulse Separation: Coincident to repetition rate period.

This system has been checked out by using it to drive a  $\text{CO}_2$  laser. Comparison of the overall efficiencies of the two pulses indicates that the coupling efficiency of the RF energy into the gas is of the order of 50%.

There are two distinct systems to which the double pulse system is applicable - radicals, and metal atoms dissociated from relatively volatile molecules. The former may be investigated in the RF-DC system.

- 
2. J.F. Prince, C.B. Collins and W.W. Robertson, J. Chem. Phys. 40, 2619 (1964).



The upper laser states of the metal atoms have fast lifetimes, necessitating fast rising, intense pulses. A cross-discharge system is superior to the longitudinal discharge in rise time and stability. Consequently, a prototype cross-discharge tube, capable of double DC pulse operation, has been constructed and tested. Current pulses with rise times on the order of 10 ns and 2 kA amplitude have been generated. When the tube is filled with  $N_2$ , the well known 3771  $N_2$  laser line is observed.

Use of the RF, DC discharge system has produced OH A-state emission in  $H_2O$  but no desired B-A state emission was observed following it or the subsequent DC pulse. Further experiments will be conducted with the double DC pulse system.

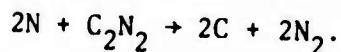
The double DC pulse system is intended primarily for investigation of the lasing potential of metal-organic compounds which have significant vapor pressures at room temperature. A 50 cm long cross-discharge tube, capable of operation of up to  $400^\circ C$  is being fabricated. If warranted, a quartz tube operable to  $700^\circ C$  or higher will be built. With this apparatus, the decomposition of metal compounds and the excitation of the metal atom will be investigated. Time resolved population studies are contemplated.

### 3. VISIBLE CHEMICAL LASER EXPERIMENTS

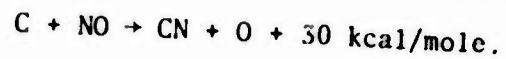
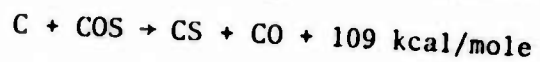
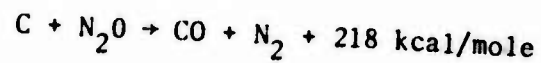
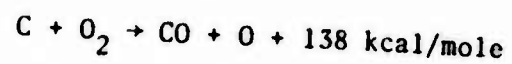
Two different methods have been applied to generate stimulated emission chemically in the visible region. The results obtained so far, however, are negative.

A. Flash Photolytic Study: During the setting up of the 1- $\mu$ sec vacuum uv ( $\lambda \geq 105$  nm) flash unit, attempts have been made to extend the observed electronic  $C^2\Pi \rightarrow A^2\Sigma^+$  and  $D^2\Sigma^+ \rightarrow A^2\Sigma^+$  NO emissions into the visible region. The two gold-coated mirrors were replaced by two high-reflectivity visible mirrors. So far no stimulated emission has been detected.

B. Transverse Fast-Flow System: A series of experiments have been carried out using a fast-flow transverse mixing system. The laser systems we investigated involve the reactions of  $C(^3P)$  atoms. The C atom was generated by mixing active nitrogen with a small amount  $C_2N_2$ , in the upper stream of the laser cavity, on the basis of the overall reaction:



$O_2$ ,  $N_2O$ ,  $COS$  and  $NO$  were introduced perpendicularly to the flow right in front of the laser cavity. The reactions of interest are:



Unfortunately, the population distribution of the products of these reactions among different electronic states are not available in the literature, no reliable estimates could be made of the gain of these systems. It should be pointed out that a bluish-red fluorescence was detected from the C + NO reaction, indicating that some CN radicals were formed in the upper electronic states.

These systems will be further investigated in the 1- $\mu$ sec flash apparatus in the near future.



APPENDIX A

QUANTITATIVE LASER MEASUREMENT OF VERY SMALL ABSORPTIONS:  
STUDIES OF THE  $O + CS \rightarrow CO(V) + S$  REACTION\*

N. Djeu

Laser Physics Branch  
Optical Sciences Division

Naval Research Laboratory  
Washington, D.C. 20375

## ABSTRACT

An intracavity laser technique has been developed to detect quantitatively very small absorptions by measurements of the laser oscillation range. The technique has been applied to the measurement of the absolute densities of the individual vibrational levels of CO produced from the reaction between O and CS in a fast flow reactor prior to any significant relaxation. Optical losses (or gains) as small as one hundredth of one percent were detectable with the present apparatus. The detectivity may be further improved by an order of magnitude with lower loss optics and a more stable laser.

## I. INTRODUCTION

A number of papers recently have reported on the dramatic enhancement in the detectivity of optical loss (or gain) obtained with the placement of the absorbing (or amplifying) medium inside a laser cavity. The experiments can be broadly categorized into two types: those using a gas laser in the infrared<sup>(1,2)</sup> and those with tunable dye lasers in the visible<sup>(3-7)</sup>. The two classes of experiments, while similar in spirit, differ considerably in the mechanics of data acquisition and interpretation. The dye laser intracavity studies are of great interest mainly because of the tunability of the device. But thus far its usefulness has been limited only to the qualitative identification of spectra. The gas laser experiments, in contrast, readily lend themselves to a quantitative analysis of the results. It is the purpose of this paper

1. N. Djeu, H.S. Pilloff, and S.K. Searles, *Appl. Phys. Letters* 18, 538 (1971).
2. S.K. Searles and N. Djeu, *IEEE J. Quantum Electronics* 9, 116 (1973).
3. N.C. Peterson, M.J. Kurylo, W. Braun, A.M. Bass, and R.A. Keller, *J. Opt. Soc. Am.* 61, 746 (1971).
4. R.A. Keller, E.F. Zalewski, and N.C. Peterson, *J. Opt. Soc. Am.* 62, 319 (1972).
5. R.J. Thrash, H. von Weyssenhoff, and J.S. Shirk, *J. Chem. Phys.* 55, 4659 (1971).
6. T.W. Hansch, A.L. Schawlow and P.G. Toschek, *IEEE J. Quantum Electronics* 8, 802 (1972).
7. G.H. Atkinson, A.H. Laufer and M.J. Kurylo, *J. Chem. Phys.* 59, 350 (1973).

to explore in some depth the potential of the gas laser intracavity probing technique. Although only the CO laser has been used to date to measure the magnitude of absorption in the intracavity manner, the principles presented here should apply equally well in conjunction with other cw gas lasers.

As an example of the kind of experiments that became possible with gas laser intracavity probing, the vibrational distribution of CO produced from the  $O + CS \rightarrow CO + S$  reaction has been studied in a flow system. The vibrational energy partitioning of the CO product from that reaction has received considerable attention lately as a result of its role in the related chemical laser<sup>(8-10)</sup>. There have been several previous attempts to characterize that partitioning<sup>(11-13)</sup>. Hancock and his co-workers made the first determination of the initial vibrational distribution by observing the overtone chemiluminescence from a relaxed distribution and then extrapolating back by making allowances for the various quenching processes. Their data yielded a skewed bell-shaped distribution with its maximum at  $V = 13$  and dropping to nearly zero at  $V = 5$  and  $V = 16$ . They subsequently obtained a similar set of results by probing a flash photolyzed mixture of  $O_2$  and  $CS_2$  with a cw CO laser beam. They noted, however, that the errors became very large in the chemiluminescence experiment for  $V \leq 7$ .<sup>(14)</sup> This situation was not improved by the laser probing experiment since their laser could only be operated above the (5,4) band. Shortly after Smith's group completed their studies, Tsuchiya, et al investigated the emission on the fundamental CO bands following a pulsed discharge in mixtures containing  $O_2$  and  $CS_2$ . In sharp contradiction to Hancock's findings, they came to the conclusion that the lowest CO vibrational levels were highly populated by the chemical reaction. In view of these conflicting reports, it appeared worthwhile to examine the problem anew. In the present work, CO was produced by mixing O and CS in a fast flow reactor at such a low pressure that its vibrational distribution was essentially unrelaxed. The CO absorption (or amplification) was measured on the (1,0) band through the (17, 16) band with intracavity laser probing. The results were then analyzed to give the absolute concentration of each of the vibrational levels from  $V = 0$  to  $V = 16$ .

8. C. Wittig, J.C. Hassler and P.D. Coleman, J. Chem. Phys. 55, 5523 (1971).
9. S.K. Searles and N. Djeu, Chem. Phys. Letters 12, 53 (1971).
10. W.Q. Jeffers, C.E. Wiswall, J.D. Kelley and R.J. Richardson, Appl. Phys. Letters 22, 587 (1973).
11. G. Hancock and I.W.M. Smith, Trans. Faraday Soc. 67, 2586 (1971).
12. G. Hancock, C. Morley and I.W.M. Smith, Chem. Phys. Letters 12, 193 (1971).
13. S. Tsuchiya, N. Nielsen and S.H. Bauer, J. Phys. Chem. 77, 2455 (1973).
14. G. Hancock, B.A. Ridley and I.W.M. Smith, J. Chem. Soc. (Faraday Trans. 1) 68, 2117 (1972).

## II. METHOD

The idea of intracavity probing grew out of the knowledge that the output of a laser operating just above threshold is very sensitive to small changes in its overall gain. To a good approximation, the output power of such a laser is proportional to the excess gain it has over the cavity loss. It is reasonable to expect a similar result to hold if the small change in the overall gain comes from a separate medium in the same laser cavity. Crudely then, if the gain of the laser is kept stably at about 0.1% above cavity loss, one can hope to observe an appreciable effect when an intracavity sample with 0.01% gain or loss on the same line is introduced. In practice the change in the laser power output due to the presence of the sample depends in a complicated fashion on the saturation behavior of both the laser and the sample. Therefore it is not a convenient parameter to follow when quantitative information is desired. Instead, the intracavity probing technique presented here is based on measurements of a quantity known as the laser oscillation range.

Figure 1 illustrates graphically the effect of a perturbing sample on the operation of a single mode frequency tuned gas laser in a low gain situation ( $\lesssim 10\%$ ). The large bell shaped curve labeled  $g(\nu)$  is the laser gain profile as a function of frequency, and the horizontal line  $\ell$  denotes the cavity loss. The laser is seen to have net gain between the frequencies  $\nu_0 - \Delta\nu/2$  and  $\nu_0 + \Delta\nu/2$ . The triangular markers on the frequency axis represent the cavity modes. They appear at intervals of  $C/2L$  where  $C$  is the velocity of light and  $L$  the cavity length. The two-way arrows just above them indicate that they will move back and forth continuously along the frequency axis as the cavity length is changed. For an increase in cavity length equal to half a wavelength the frequency of each mode is diminished by  $C/2L$ . When one of the cavity modes falls within the range of net gain, in this example  $\nu_m$ , the laser will oscillate at the frequency of that particular mode. If  $C/2L > \Delta\nu$ , the laser can oscillate on only one cavity mode at any instant. As the cavity mode moves across the region of net gain, a single mode frequency tuning curve resembling the lower power output trace is produced. Accordingly, the frequency interval  $\Delta\nu$  is known as the laser oscillation range. Now if an additional gain is introduced into the cavity in the form of  $g'(\nu)$ , the region of net gain will be broadened to  $\Delta\nu'$ . Correspondingly a new frequency tuning curve with  $\Delta\nu'$  as the oscillation range will be observed. (The opposite effect of a sample loss should be equally obvious.) It will be shown now that under the conditions of interest  $g'(\nu_0)$  is related to  $\Delta\nu$ ,  $\Delta\nu'$ , and  $\ell$  in a straightforward manner.

The frequency dependence for a laser transition with mixed Doppler and pressure broadening can be written as <sup>(15)</sup>

15. A.C.G. Mitchell and M.W. Zemansky, Resonance Radiation and Excited Atoms (Cambridge U.P., London, 1961).

$$\alpha(\nu) = \frac{\alpha'}{\sqrt{\pi}} \int_0^{\infty} \exp\left(-ax - \frac{x^2}{4}\right) \cos\left(\frac{2\sqrt{\ln 2}(\nu - \nu_0)x}{\Delta \nu_D}\right) dx \quad (1)$$

with

$$a = \frac{\Delta \nu_P + \Delta \nu_R}{\Delta \nu_D} \sqrt{\ln 2}$$

where  $\alpha'$  is the line center gain in the limit of Doppler broadening,  $\nu_0$  the line center frequency and  $\Delta \nu_P$ ,  $\Delta \nu_R$ , and  $\Delta \nu_D$  are the pressure broadened, radiation broadened, and Doppler broadened linewidths respectively. Near the peak of the gain profile, one can expand the cosine term in the integral to obtain

$$\begin{aligned} \alpha(\nu) &\approx \frac{\alpha'}{\sqrt{\pi}} \int_0^{\infty} \exp\left(-ax - \frac{x^2}{4}\right) \left(1 - \frac{2\sqrt{\ln 2}(\nu - \nu_0)x}{\Delta \nu_D}\right) dx \\ &= \alpha' \exp(a^2) \operatorname{erfc}(a) \\ &\quad - 4\alpha' \sqrt{\ln 2} \left( (1 + 2a^2) \exp(a^2) \operatorname{erfc}(a) - \frac{2a}{\sqrt{\pi}} \right) \frac{(\nu - \nu_0)^2}{\Delta \nu_D^2} \\ &\equiv \alpha_0 - 4\alpha_2 (\nu - \nu_0)^2 \end{aligned} \quad (2)$$

where the last step defines the parameters  $\alpha_0$  and  $\alpha_2$ . In the absence of the sample, the laser oscillation range  $\Delta \nu^0$  is seen from Fig. 1 and Eq. 2 to obey

$$l = (\alpha_0 - \alpha_2 \Delta \nu^0{}^2) z \quad (3)$$

where  $z$  is the active length of the laser medium. In the limit that the linewidth of the perturbing medium is much greater than  $\Delta \nu$ , the introduction of the sample results in a new oscillation range  $\Delta \nu'$  given by

$$l = g'(\nu_0) = (\alpha_0 - \alpha_2 \Delta \nu'^2) z. \quad (4)$$

Solving Eqs. (3) and (4) together with the approximation that  $l \approx \alpha_0 z$  (near threshold condition) gives

$$g'(v_0) = (\Delta v^{-2} - \Delta v^2) \frac{\alpha_2}{\alpha_0} l \quad (5)$$

In the limit that the gain profile is purely Doppler broadened, Eq. (5) becomes

$$g'(v_0) = (\Delta v^{-2} - \Delta v^2) \frac{l \ln 2}{\Delta v_D^2} \quad (6)$$

In practice, the laser oscillation range is an easily measurable parameter. One simply applied a linear scan of the cavity length with time for a displacement greater than half a wavelength. The single mode frequency tuned output would then show repetitions of the tuning curve. The periodicity of the output is exactly  $C/2L$ , thus serving as a scale for the measurement of  $\Delta v$  (see box labeled "oscilloscope" in Fig. 2). To determine  $g'(v_0)$  absolutely it is necessary to calibrate the apparatus internally with a known amount of absorber initially. But the quantity  $\alpha_2 l / \alpha_0$  generally can be surmised to a good degree of accuracy, making rough estimates of  $g'(v_0)$  possible without the calibration procedure. The latter was in fact the approach taken in Refs. (1) and (2), but in this work the exact values of  $\alpha_2 l / \alpha_0$  were measured. The validity of Eq. (5) was assumed in the earlier work; in the present study it was firmly established through a series of experiments.

### III. APPARATUS

For the effective use of the laser oscillation range technique, one must have a constant gain medium and a stable laser cavity. Consequently, the apparatus described below incorporates some design features which are not commonly found in the usual laboratory CO laser systems. A simplified schematic of the apparatus is given in Fig. 2. The laser tube had an active length of 1.5 m and was liquid nitrogen cooled over that entire region. Gases were admitted into the tube near the two ends and pumped out at the middle. To minimize fluctuations in the gain of the laser medium, a large volume was interposed between the laser tube and the vacuum pump, and a current regulator was used in series with the power supply. When a mixture of He, N<sub>2</sub>, Xe, and CO was used, single-line operation was possible down to the (1,0) band.<sup>(16)</sup> The laser cavity, formed by a 2% transmitting curved mirror and a 300 lines/mm grating, was mounted on a steel I-beam which in turn was floated on four air bags. The laser tube and the reactor were secured to the bench top without touching the suspended I-beam. This



simple scheme of vibration isolation proved to be quite satisfactory for the purpose of the present experiment.

Single transverse mode operation was achieved by closing down the variable iris in front of the output mirror. The mirror itself was mounted on a piezoelectric transducer which converts an applied voltage into a proportional extension of the element. When a linear ramp generator was used to drive the PZT, the horizontal axis of the signal observed on the oscilloscope could be considered as frequency as well as time. As pointed out earlier, for a change in cavity length equal to one half the laser wavelength, the power tuning curve repeats itself. The frequency difference between successive modes,  $C/2L$ , then served as a convenient reference for the measurement of  $\Delta\nu$ .

The reactor, near the grating end of the cavity, was an aluminum box of rectangular cross section (10.2 cm x 3.0 cm) fitted with Brewster's angle windows. It was divided into four channels just upstream from the optical axis, as shown in the sketch in Fig. 3. The two inner ones were used for the reactants O and CS respectively. The CS channel terminated in a Teflon injector comprised of 15 evenly spaced 3 mm diameter holes aimed in the direction of the optical axis. The outer channels permitted the flow of some inert gas to minimize the effect of the walls. The O atoms and CS radicals were generated in glass discharge tubes located immediately outside the metal reactor. To reduce the possibility of the discharges trailing downstream, the entire inside of the reactor had been coated with Teflon. Not shown in Fig. 2 are inlet ports opposite the Brewster's angle windows used for the purging of those protruded regions. A 150 C.F.M. mechanical pump provided the necessary fast flow of the reacting mixture across the optical axis.

#### IV. CALIBRATIONS

A direct verification of the validity of Eq. (5) is possible if sufficient CO in any vibrational level with a known concentration can be introduced into the reactor. This is obviously the case for ground state CO so long as the probe laser can be made to oscillate on the (1,0) band. However, with the sensitivity of the present apparatus even the thermal population of CO in  $V = 1$  would adequately produce the needed absorption. In fact, the latter was chosen instead of the ground state molecules since an accurate determination of the appropriate concentrations was much easier for CO in  $V = 1$ .

Aside from putting the basic premise of the laser oscillation range method to a test, a calibration run on the (2,1) band would also yield the value of cavity loss for that band. However, for the wide spectral

range covered in this experiment ( $\sim 1 \mu\text{m}$ ), one cannot expect the cavity loss to be a constant. This is due to the wavelength dependence of such lossy elements as the diffraction grating and the variable iris. Therefore one must further correlate the cavity loss for the (2,1) band with that for the others. This was done quite simply by measurements of the laser lineshape and inversion ratio for all the bands concerned.

For the test run on the (2,1) band absorption of CO at room temperature the P(7) line was used. Near threshold oscillation was obtained by adjusting the partial pressure of CO in the gain tube or by changing the discharge current. The laser oscillation range was read off the oscilloscope directly. Then upon the admittance of a known amount of CO into the reactor, the new oscillation range was noted. The difference between  $\Delta\nu'$  and  $\Delta\nu''$  was taken and plotted against the CO pressure. A set of data with each representing a single pair of measurements is shown in Fig. 4. In obtaining these points,  $\Delta\nu$  was varied slightly so that  $\Delta\nu'$  at each CO pressure was only a few MHz. That the points do fall on a straight line are an indication of the errors involved in taking a single set of measurements.

The magnitude of line center absorption can be calculated from the following formula for optical gain on the P(J) line in the (V, V-1) band:

$$\alpha^V(J) = \frac{hc}{kT} \sqrt{\frac{M}{2\pi kT}} \frac{\lambda^3 A(V)}{8\pi} J \times \left[ N_V B_V \exp\left(-F_V(J-1) \frac{hc}{kT}\right) - N_{V-1} B_{V-1} \exp\left(-F_{V-1}(J) \frac{hc}{kT}\right) \right] \quad (6)$$

where  $A(V)$  is the transition probability for the band,  $N_V$  and  $N_{V-1}$  are the densities of the upper and lower vibrational levels respectively,  $B_V$  is the rotational constant for the Vth vibrational level, and  $F_V(J) = B_V J(J+1)$ . For CO at room temperature, the density of the upper vibrational level may be set equal to zero. Then one easily calculates an absorption coefficient of  $1.3 \times 10^{-16} \text{ N}_1 \text{ cm}^{-1}$  for the P(7) line in the (2,1) band. At  $T = 298^\circ\text{K}$ , the fraction of CO molecules in the  $V = 1$  level is  $0.33 \times 10^{-4}$ , making the pressure dependent absorption  $1.3 \times 10^{-4} \text{ cm}^{-1} \text{ torr}^{-1}$  (so long as the line remains Doppler broadened). The distance between the two Brewster's windows on the reactor was 17 cm, so the roundtrip loss due to the "cold" CO on the relevant line was  $0.44\% \text{ torr}^{-1}$ . Using this number, one calculates from the slope of the line in Figure 4  $\alpha_2/\alpha_0 = 8.8 \times 10^{-18} \text{ sec}^2$ . The ratio  $\alpha_0/\alpha_2$  is a function of the Doppler broadened and pressure broadened widths of the laser line in the gain medium. Those quantities

can be deduced from a measurement of the oscillation ranges for a number of vibration-rotation transitions in the band. The exact procedure whereby they are extracted can be found in Ref. 17. In the present instance,  $\alpha_0/\alpha_2$  was found to be  $1.1 \times 10^{16} \text{ sec}^{-2}$ , which gave a cavity loss of 9.7% on the (2,1) band.

The value for cavity loss changes with the wavelength of the laser transition. The diffraction grating used as one end mirror was blazed for 4  $\mu\text{m}$ ; hence it reflected with lower efficiency for the higher lying bands. Furthermore, the diffraction loss due to the iris at a fixed diameter is also wavelength dependent, becoming greater for longer wavelength<sup>(18)</sup>. The combination of these effects produced a substantial change in total cavity loss over the wide range of bands employed. Fortunately, it was possible to determine that variation through a series of correlation of oscillation ranges. The same procedure referred to earlier which yields the Doppler and pressured broadened widths also gives the inversion ratio for the band. In fact, it was shown in Ref. 17 that extremely accurate values of the inversion ratio could be obtained with that method. It is clear that once the lineshapes and the inversion ratios are known for two adjacent bands, the ratio between their respective cavity losses follows from the magnitude of the oscillation ranges in the corresponding bands. Thus the cavity losses can be correlated in pairwise fashion for all the bands needed in the experiment. Because of the high accuracy with which the inversion ratios could be determined, the cumulative error over many bands was still tolerable. For the particular iris diameter used in the present experiment, the cavity loss was found to increase by as much as a factor of two from (1,0) to (16,15) (with an uncertainty of the order of 10%).

#### V. STUDIES OF $\text{O} + \text{CS} \rightarrow \text{CO}(\text{V}) + \text{S}$

The aim of the present investigation was to measure the absorption (or amplification) due to a steady state concentration of vibrationally unrelaxed CO molecules produced from the reaction between  $\text{O} + \text{CS}$  in a flow apparatus. The major mechanism for the degradation of the initial vibrational distribution is V-V exchange collisions of the type  $\text{CO}(\text{V}) + \text{CO}(\text{V}') \rightarrow \text{CO}(\text{V}+1) + \text{CO}(\text{V}'-1)$ . The probability for  $\text{CO}(\text{V}) + \text{CO}(0) \rightarrow \text{CO}(\text{V}-1) + \text{CO}(1)$  is known to be very high.<sup>(19-21)</sup> One expects an even larger cross section for V-V exchange between two CO molecules both in high vibrational levels. Gas flow measurements on the present

18. T. Li, Bell System Tech. J. 44, 917 (1965).

19. G. Hancock and I.W.M. Smith, Appl. Optics 10, 1827 (1971).

20. J.C. Stephenson, Appl. Phys. Letters 22, 576 (1973).

21. H.T. Powell, to be published in J. Chem. Phys.

apparatus with air gave a linear flow rate of  $19 \text{ msec}^{-1}$  in the reactor. This implied a residence time of 0.3 msec for an average CO product molecule before crossing the optical axis. Therefore CO concentrations up to  $10^{12} \text{ cm}^{-3}$  per vibrational level could be tolerated even if V-V exchange occurred on every collision. A quick calculation showed that such densities should be within the limits of detection of the present system.

The reagents  $\text{O}$  and  $\text{CS}_2$  were produced from electric discharges in  $\text{He-O}_2$  and  $\text{Ar-CS}_2$  respectively. The  $\text{O}_2$  discharge was d.c. powered and maintained at 100 mA, while the  $\text{CS}_2$  discharge was supplied by a neon sign transformer. Flow rates of  $1.7 \text{ m-mole sec}^{-1}$  He,  $0.14 \text{ m-mole sec}^{-1}$   $\text{O}_2$ , and  $0.22 \text{ m-mole sec}^{-1}$  Ar ( $\text{CS}_2$  carrier) were used throughout the experiment. For the lowest CO vibrational levels to be detectable, a  $\text{CS}_2$  flow rate of  $\sim 0.01 \text{ m-mole sec}^{-1}$  was required.

The difference of oscillation ranges squared,  $\Delta v'^2 - \Delta v^2$ , was measured on about half a dozen vibration-rotation transitions in each band from (1,0) to (17,16). This was accomplished by momentarily opening a metering needle valve in the  $\text{CS}_2$  line to a fixed position. Depending on whether a particular transition exhibited gain or loss, the smaller of  $\Delta v'$  and  $\Delta v$  was always kept to a value of less than 10 MHz. Two or three measurements were taken on each transition and the results were averaged. The scatter on each data point was typically in the neighborhood of 10%.

To keep the Brewster's windows free from deposits, Ar was admitted in through ports opposite the windows at the rate of  $0.07 \text{ m-mole sec}^{-1}$  on each side. The flow also served to prevent the diffusion of CO product molecules into those regions, although the effect was noticeable only on the (1,0) band.

Among the first studies performed was an evaluation of the effectiveness of the discharge in the  $\text{Ar-CS}_2$  line. The observation was made that the extinction of the discharge reduced the signal by a factor of about 3 at a  $\text{CS}_2$  flow rate of  $0.017 \text{ m-mole sec}^{-1}$ . The residual signal was apparently due to CO produced from the successive reactions  $\text{O} + \text{CS}_2 \rightarrow \text{CS}^* + \text{SO}$  and  $\text{O} + \text{CS}^* \rightarrow \text{CO} + \text{S}$ .<sup>(11)</sup> Since the direct reaction  $\text{O} + \text{CS}_2 \rightarrow \text{CO} + \text{S}$  consumed O atoms faster than the two-step reaction, it was concluded that with the use of the discharge more than two thirds of the CO detected came from the former source. Furthermore, the relatively long transit time (tens of msec) between the discharge and the nozzle insured that the CS entering the reaction region were predominantly in the vibrational ground state, even if a good fraction had been excited into the higher levels initially by the discharge.

11. G. Hancock and I.W.M. Smith, Trans. Faraday Soc. 67, 2586 (1971).

22. R.J. Richardson, H.T. Powell, and J.D. Kelley, to be published in J. Chem. Phys.



The extent of vibrational quenching resulting from collisions with the wall was easily discernable in the present type of experiment. The  $\text{CO}(V)$  distribution remained constant only for Ar flow rates in excess of  $\sim 0.05$  m-mole  $\text{sec}^{-1}$  in each of the two outside channels. With reduced Ar flows there was a clear shift of the distribution towards  $V = 0$ . Although an estimate of the probability for  $\text{CO}(V) + \text{wall} \rightarrow \text{CO}(V') + \text{wall}$  seemed out of reach, rough calculations using the known linear flow rate and diffusion constants indicated that wall deactivation must have been very efficient. To be free from the effect of the walls, an Ar flow rate of  $0.65$  m-mole  $\text{sec}^{-1}$  per channel was used in subsequent studies, raising the total pressure in the reactor to  $1.1$  torr.

The question of whether V-V exchange might have caused any appreciable relaxation of the initial vibrational distribution under the circumstances was answered by varying the  $\text{CS}_2$  flow rate. It was found that doubling the  $\text{CS}_2$  flow rate to  $0.035$  m-mole  $\text{sec}^{-1}$  essentially doubled the signal on each of the bands. This seemed to be convincing proof that the concentration of CO present was sufficiently low to make V-V exchange a negligible process. From the data collected in Ref. 19 it was decided that V-T relaxation was also unimportant under the operating conditions. Finally, with a radiative lifetime of  $\sim 4$  msec for the highest vibrational levels populated, the modification of the distribution caused by radiative decay during the  $0.3$  msec residence time was clearly minor.

A perplexing feature in the observed distribution was a sharp jump in concentration for  $\text{CO}(V=0)$ . As one approached the lowest bands from above, there was a clear break in the magnitude as well as sign of the measured absorption when  $(1,0)$  was reached. Furthermore, unlike the signals on the other bands, the  $(1,0)$  band absorption fluctuated from day to day beyond the limits of experimental uncertainty. At first it was thought that perhaps wall quenching was still persisting to a small degree. But upon further investigation it was discovered that with the  $\text{CS}_2$  completely shut off a "gain" of comparable magnitude could be produced by turning off the discharge in the  $\text{He-O}_2$  line. It was concluded that the ground state molecules were probably produced from reactions between discharged oxygen and some carbonaceous deposits on the reactor wall. However, in the interest of presenting the results in as untempered a form as possible, no correction was made for this extraneous effect.

## VI. ANALYSIS OF RESULTS

The measured oscillation ranges were converted into gain or loss through the use of Eq. (5) with the previously determined cavity loss for each band. In principle, for each band the inversion ratio could be deduced from the relative absorptions of its vibration-rotation lines as

mentioned earlier. Then a distribution could be generated from those ratios. But in practice, unless extremely accurate experimental data were available, the relative densities for the two ends of the distribution determined in this manner would be in large error. To circumvent this difficulty, an alternative scheme was used in which a least square analysis was done on all the bands simultaneously.

With the assumption that the errors have a Gaussian distribution, the vibrational level densities are given by

$$\sum_{VJ} \frac{X_V^V(J) - \alpha_V^V(J)}{\alpha_V^V(J)^2} \frac{\partial \alpha_V^V(J)}{\partial N_i} = 0 \quad (7)$$

where  $X_V^V(J)$  is the measured absorption on the  $P(J)$  line in the  $(V, V-1)$  band,  $\sigma_V^V(J)^2$  the standard deviation for that quantity and  $\alpha_V^V(J)$  is given in Eq. (6). The indices  $V$  and  $J$  run through all the vibration-rotation lines covered in the experiment. The index  $i$  takes on the values 0 through 16 in the present case, and Eq. (7) is in fact a set of 17 simultaneous linear equations. In the laser oscillation range method, the standard deviation  $\sigma_V^V(J)^2$  is proportional to  $X_V^V(J)$  with approximately the same constant of proportionality for all  $V$  and  $J$ . One can therefore rewrite Eq. (7) as

$$\sum_{VJ} \left( 1 - \frac{\alpha_V^V(J)}{X_V^V(J)} \right) \frac{\partial \alpha_V^V(J)}{\partial N_i} = 0 \quad (8)$$

In order to use Eq. (8) one must know the temperature in the sample which appears in Eq. (6). A thermocouple placed on the optical axis inside the reactor showed no rise in temperature with the ignition of the discharges in He-O<sub>2</sub> and Ar. It registered an increase of 2°C when CS<sub>2</sub> was added to the Ar stream. Therefore a temperature of 300°K was used in solving Eq. (8).

The results for a CS<sub>2</sub> flow rate of 0.017 m-mole sec<sup>-1</sup> after normalization by  $N_{12}$  are shown in Fig. 5. The absolute concentration of CO( $V=12$ ) in this case is  $2.5 \times 10^{12}$  cm<sup>-3</sup>. It is worth noting that under the present scheme of data reduction it is possible to obtain negative values for the level densities. In view of this consideration, the fact that the two ends of the distribution in Fig. 5 only come close to zero but not beyond it gives one some confidence in the reliability of the measured data. In particular, the low value of  $N(16)$  given by the analysis is confirmed by the observed lack of signal on (17,16). From the evidence presented in the last section the vibrational distribution given in Fig. 5, with the exception of  $N(0)$ , must be regarded as a good approximation of the one initially produced by the chemical reaction.



## VII. DISCUSSION

The distribution in Fig. 5 agrees well with those given by Hancock et al, especially when account is taken of the large error limits placed on the latter.<sup>(14)</sup> The present results seem to be slightly shifted towards lower  $V$  by one to two quanta in comparison. This discrepancy, if real, could have been caused by a small but finite amount of V-V exchange still persisting in the present experiment. In any event, there is now strong evidence that the reaction between O and CS does produce only a negligible fraction of CO in  $V \lesssim 5$ .

During the preparation of this manuscript it was learned that yet another study had been completed on the present reaction by H.T. Powell and J.D. Kelley.<sup>(23)</sup> In their work a CS<sub>2</sub>-O<sub>2</sub> mixture following the application of a pulsed discharge was probed using the output of a cw CO laser. Measurements were made on the (3,2) through (20,19) bands. The distribution obtained appeared to support the findings of Tsuchiya et al for the lowest  $V$  levels. However, they made the disturbing observation that under certain conditions  $V = 2$  and  $V = 3$  were populated at a faster rate during a brief initial period, indicating that a second reaction might have been contributing to the formation of CO in the low levels. They suggested  $C + O_2 \rightarrow CO + O$  as a possible detracting reaction. Since a pulsed discharge was also used in Tsuchiya's experiment, one suspects that the low  $V$  CO molecules detected in both cases may have come from reactions other than  $O + CS \rightarrow CO + S$ .

The laser oscillation range technique developed here is unmatched in its sensitivity for the quantitative detection of small absorptions. Compared to conventional absorption or emission spectroscopy, the resolution of the laser method is orders of magnitude better. Thus it should be particularly useful in cases where the transitions of interest may lie very close to other absorbing or emitting lines. The present work demonstrates that a detectivity of a few hundredths of a percent is possible with a cavity loss of 10%. The use of fewer Brewster windows (one is the minimum required) and higher reflecting end mirrors (perhaps the substitution of the grating by a prism) could reduce that loss by a factor of two to three. There is also much room for improving the stability of the gain medium, which sets the ultimate limit on the technique. It is believed that with these and other modifications the measurement of absorptions as small as a few thousandths of one percent should be feasible.

14. G. Hancock, B.A. Ridley and I.W.M. Smith, J. Chem. Soc. (Faraday Trans. II) 68, 2117 (1972).

23. H.T. Powell and J.D. Kelley, to be published, J. Chem Phys.

#### ACKNOWLEDGEMENTS

The author wishes to thank J.R. Airey and W.S. Watt for their helpful comments on the manuscript.

#### REFERENCES

1. N. Djeu, H.S. Pilloff, and S.K. Searles, Appl. Phys. Letters 18, 538 (1971).
2. S.K. Searles and N. Djeu, IEEE J. Quantum Electronics 9, 116 (1973).
3. N.C. Peterson, M.J. Kurylo, W. Braun, A.M. Bass, and R.A. Keller, J. Opt. Soc. Am. 61, 746 (1971).
4. R.A. Keller, E.F. Zalewski, and N.C. Peterson, J. Opt. Soc. Am. 62, 319 (1972).
5. R.J. Thrash, H. von Weyssenhoff and J.S. Shirk, J. Chem. Phys. 55, 4659 (1971).
6. T.W. Hansch, A.L. Schawlow and P.G. Toschek, IEEE J. Quantum Electronics 8, 802 (1972).
7. G.H. Atkinson, A.H. Laufer and M.J. Kurylo, J. Chem. Phys. 59, 350 (1973).
8. C. Wittig, J.C. Hassler and P.D. Coleman, J. Chem. Phys. 55, 5523 (1971).
9. S.K. Searles and N. Djeu, Chem. Phys. Letters 12, 53 (1971).
10. W.Q. Jeffers, C.E. Wiswall, J.D. Kelley and R.J. Richardson, Appl. Phys. Letters 22, 587 (1973).
11. G. Hancock and I.W.M. Smith, Trans. Faraday Soc. 67, 2586 (1971).
12. G. Hancock, C. Morley and I.W.M. Smith, Chem. Phys. Letters 12, 193 (1971).
13. S. Tsuchiya, N. Nielsen and S.H. Bauer, J. Phys. Chem. 77, 2455 (1973).
14. G. Hancock, B.A. Ridley and I.W.M. Smith, J. Chem. Soc. (Faraday Trans. II) 68, 2117 (1972).
15. A.C.G. Mitchell and M.W. Zemansky, Resonance Radiation and Excited Atoms (Cambridge U.P., London, 1961).

16. N. Djeu, Appl. Phys. Letters 23, 309 (1973).
17. N. Djeu and S.K. Searles, IEEE J. Quantum Electronics 8, 811 (1972).
18. T. Li, Bell System Tech. J. 44, 917 (1965).
19. G. Hancock and I.W.M. Smith, Appl. Optics 10, 1827 (1971).
20. J.C. Stephenson, Appl. Phys. Letters 22, 576 (1973).
21. H.T. Powell, to be published, J. Chem. Phys.
22. R.J. Richardson, H.T. Powell, and J.D. Kelley, to be published, J. Phys. Chem.
23. H.T. Powell and J.D. Kelley, to be published, J. Chem. Phys.

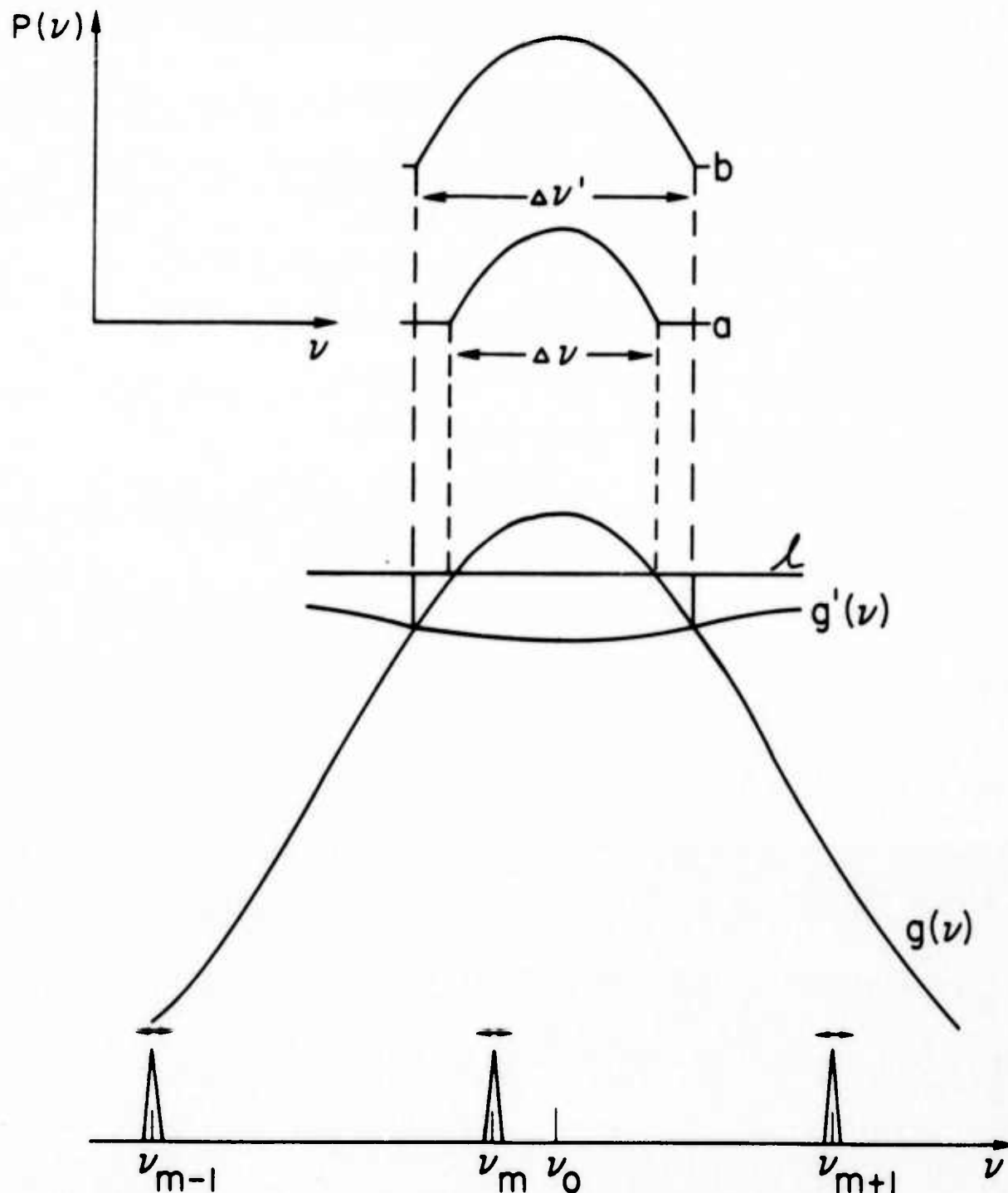


Fig. A-1 - Schematic of the effect of a perturbing gain on the laser oscillation range. The lower portion of the figure shows the threshold condition of the laser. Note that  $g(\nu)$  has the  $\nu$  axis as baseline, whereas  $g'(\nu)$  is drawn inverted with the cavity loss  $l$  as its baseline. In the upper part,  $P(\nu)$  denotes the single mode power output at  $\nu$ . The tuning curves b and a with and without the sample gain  $g'(\nu)$  have nonzero output only in the regions  $\Delta\nu'$  and  $\Delta\nu$  respectively.

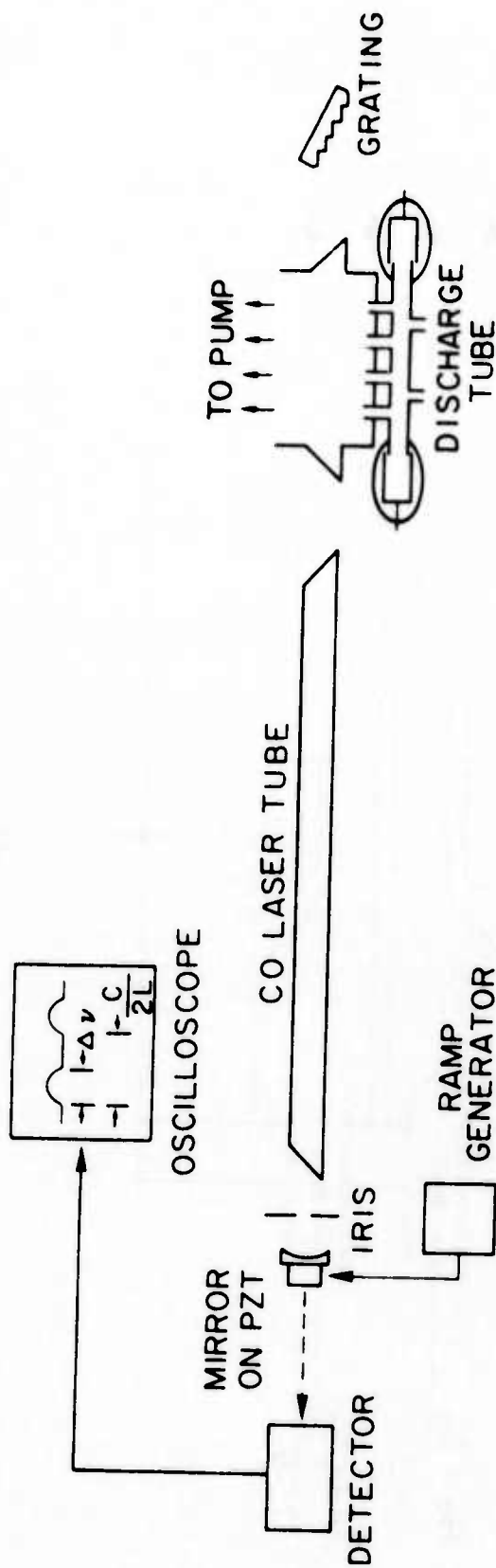


Fig. A-2 - Schematic of the Apparatus

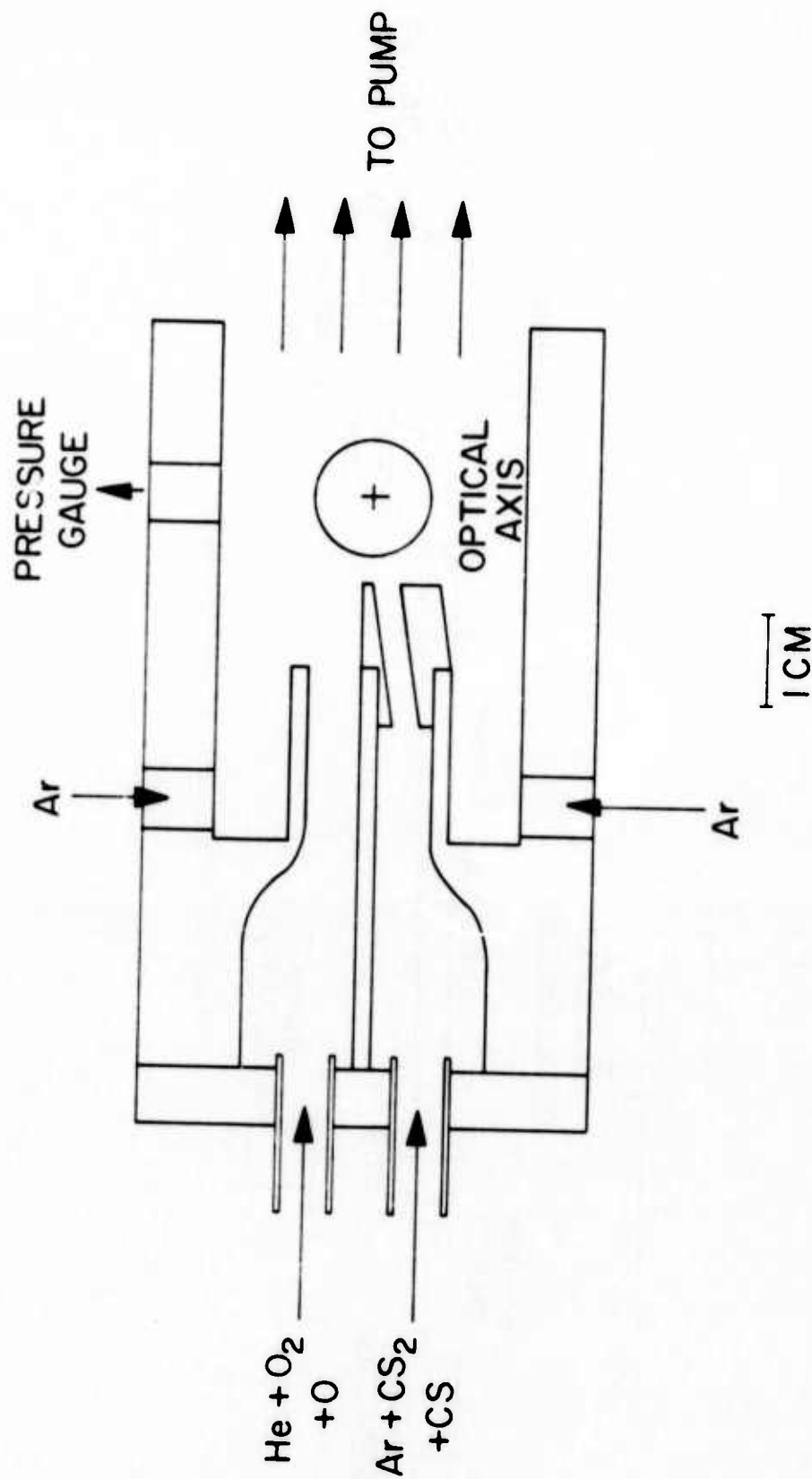


Fig. A-3 - Details of the Reactor



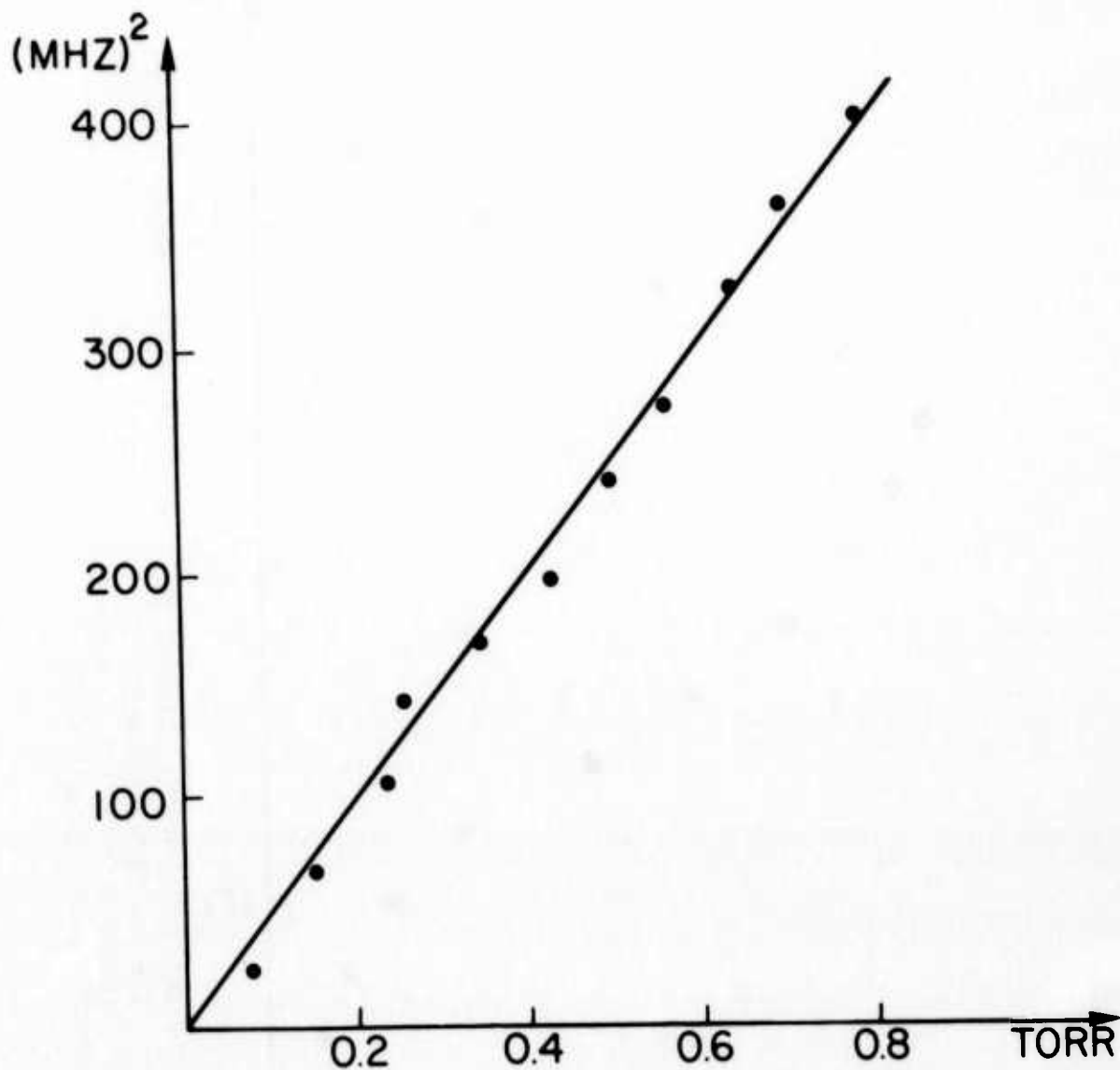


FIG. A-4 - CALIBRATION CURVE ON THE P(7) LINE IN THE (2,1) BAND. THE MEASURED  $\Delta v^2 - \Delta v'^2$  IS PLOTTED AGAINST THE CO PRESSURE IN THE REACTOR. THE FRACTION OF CO IN (V=1, J=7) IS  $2.7 \times 10^{-6}$ .

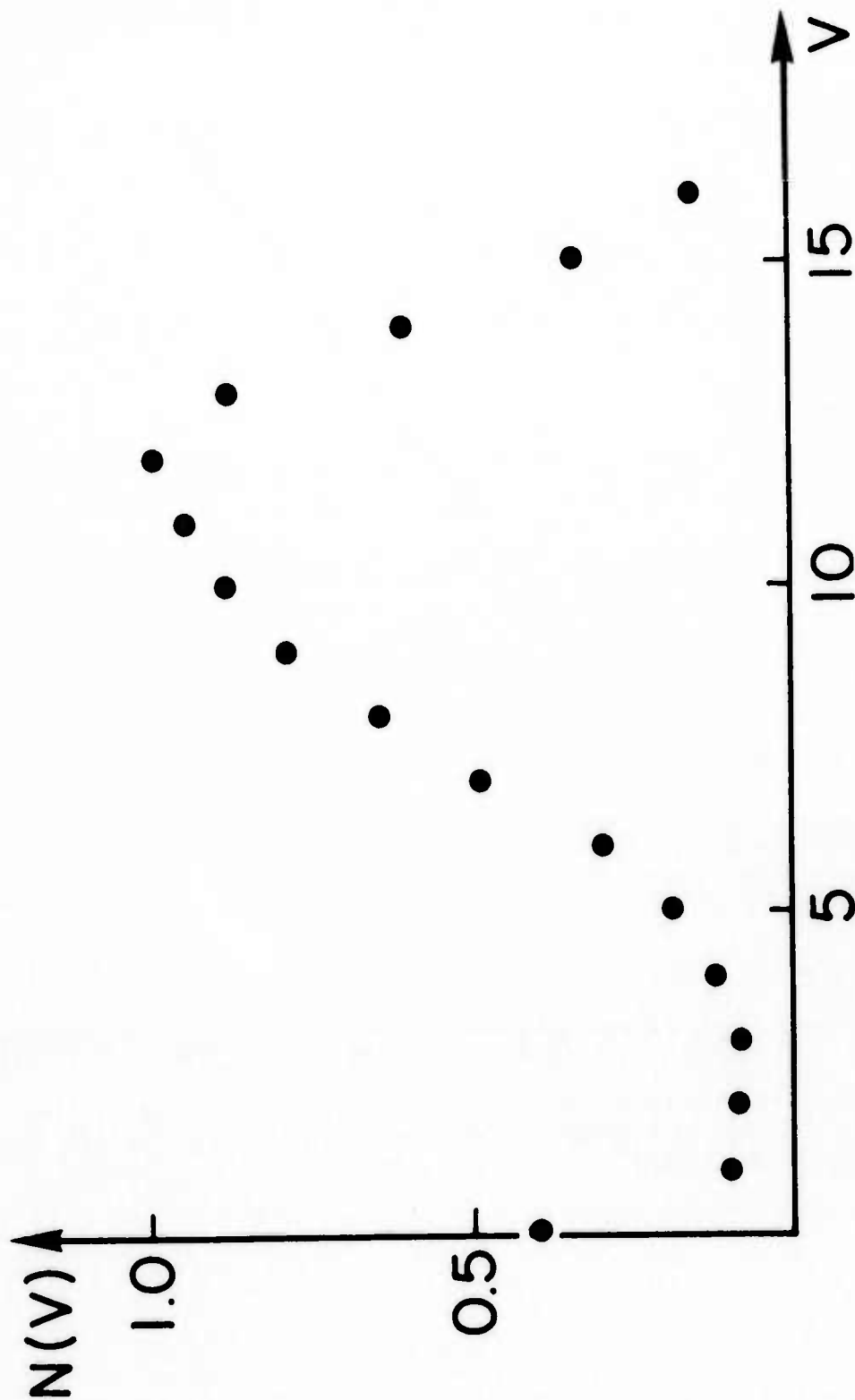


FIG. A-5 - MEASURED VIBRATIONAL DISTRIBUTION OF CO FROM THE REACTION BETWEEN O AND CS<sub>2</sub> NORMALIZED TO N(12). THE CS<sub>2</sub> FLOW RATE WAS 0.017 m-mole sec<sup>-1</sup>, AND THE CONCENTRATION OF CO IN V = 12 WAS CALCULATED TO BE 2.5 x 10<sup>12</sup> cm<sup>-3</sup>. THE POPULATION AT V = 0 WAS MOSTLY DUE TO AN EXTRANEEOUS SOURCE (SEE TEXT).